ISSN 2355-3286

ULTIMA Computing

Jurnal Sistem Komputer

Engineering | Vol. 16 | No. 2 | Page 46 - 85 | December 2024 | ISSN 2355-3286

UMN

UNIVERSITAS
MULTIMEDIA
NUSANTARA

ISSN 2355-3286

EDITORIAL ADDRESS

Universitas Multimedia Nusantara (UMN)
Jl. Scientia Boulevard
Gading Serpong
Tangerang, Banten - 15811
Indonesia
Phone. (021) 5422 0808
Fax. (021) 5422 0800
Email : ultimacomputing@umn.ac.id

Ultima Computing : Jurnal Sistem Komputer is a Journal of Computer Engineering Study Program, Universitas Multimedia Nusantara which presents scientific research articles in the field of Computer Engineering and Electrical Engineering as well as current theoretical and practical issues, including Edge Computing, Internet-of-Things, Embedded Systems, Robotics, Control System, Network and Communication, System Integration, as well as other topics in the field of Computer Engineering and Electrical Engineering. The Ultima Computing : Jurnal Sistem Komputer is published regularly twice a year (June and December) and is jointly managed by the Computer Engineering and Electrical Engineering Study Program at Universitas Multimedia Nusantara.

Call for Papers

International Journal of New Media Technology (IJNMT) is a scholarly open access, peer-reviewed, and interdisciplinary journal focusing on theories, methods and implementations of new media technology. Topics include, but not limited to digital technology for creative industry, infrastructure technology, computing communication and networking, signal and image processing, intelligent system, control and embedded system, mobile and web based system, and robotics. IJNMT is published twice a year by Faculty of Engineering and Informatics of Universitas Multimedia Nusantara in cooperation with UMN Press.

Ultimatics : Jurnal Teknik Informatika is the Journal of the Informatics Study Program at Universitas Multimedia Nusantara which presents scientific research articles in the fields of Analysis and Design of Algorithm, Software Engineering, System and Network security, as well as the latest theoretical and practical issues, including Ubiquitous and Mobile Computing, Artificial Intelligence and Machine Learning, Algorithm Theory, World Wide Web, Cryptography, as well as other topics in the field of Informatics.

Ultima Computing : Jurnal Sistem Komputer is a Journal of Computer Engineering Study Program, Universitas Multimedia Nusantara which presents scientific research articles in the field of Computer Engineering and Electrical Engineering as well as current theoretical and practical issues, including Edge Computing, Internet-of-Things, Embedded Systems, Robotics, Control System, Network and Communication, System Integration, as well as other topics in the field of Computer Engineering and Electrical Engineering.

Ultima InfoSys : Jurnal Ilmu Sistem Informasi is a Journal of Information Systems Study Program at Universitas Multimedia Nusantara which presents scientific research articles in the field of Information Systems, as well as the latest theoretical and practical issues, including database systems, management information systems, system analysis and development, system project management information, programming, mobile information system, and other topics related to Information Systems.

FOREWORD

ULTIMA Greetings!

Ultima Computing : Jurnal Sistem Komputer is a Journal of Computer Engineering and Electrical Engineering at Multimedia Nusantara University which presents scientific research articles in the field of Computer Systems as well as the latest theoretical and practical issues, including Edge Computing, Internet-of-Things, Embedded Systems, Robotics, Control Systems, Network and Communication, System Integration, and other topics in the field of Computer Engineering and Electrical Engineering.

In this December 2024 edition, Ultima Computing enters the 2nd Edition of Volume 16. In this edition there are five scientific papers from researchers, academics and practitioners in the fields of Computer Engineering and Electrical Engineering. Some of the topics raised in this journal are: Liquid Petroleum Gas (LPG) Cylinder Leak Detection Tool Using MQ-2 Sensor Based on Internet of Things (IoT), Analysis of Noise Removal Performance in Speech Signals through Comparison of Median Filter, Low FIR Filter, and Butterworth Filter: Simulation and Evaluation, Development of Cavendish Banana Maturity Detection and Sorting System Using Open Source Computer Vision and Loadcell Sensor, Air Filtration System Utilizing Biomimetic Technology and IoT for Air Quality Improvement, and Microscopic Sand Image Classification Using Convolutional Neural Networks.

On this occasion we would also like to invite the participation of our dear readers, researchers, academics, and practitioners, in the field of Engineering and Informatics, to submit quality scientific papers to: International Journal of New Media Technology (IJNMT), Ultimatics : Jurnal Teknik Informatics, Ultima Infosys: Journal of Information Systems and Ultima Computing: Journal of Computer Systems. Information regarding writing guidelines and templates, as well as other related information can be obtained through the email address ultimacomputing@umn.ac.id and the web page of our Journal here.

Finally, we would like to thank all contributors to this December 2024 Edition of Ultima Computing. We hope that scientific articles from research in this journal can be useful and contribute to the development of research and science in Indonesia.

December 2024,

Monica Pratiwi, S.ST., M.T.
Editor-in-Chief

TABLE OF CONTENT

ISSN 2355-3286

Liquid Petroleum Gas (LPG) Cylinder Leak Detection Tool Using MQ-2 Sensor Based on Internet of Things (IoT)

Hartawan Alief Nugroho Wicaksono[1], Rizky Oriza Syahda[2], Nur Syahid[3], Indri Purwita Sary[4]
[1,2,3,4] Faculty of Engineering, Singaperbangsa University Karawang, Karawang, Indonesia
[1]2010631160119@student.unsika.ac.id, [2]2010631160109@student.unsika.ac.id,
[3]2010631160099@student.unsika.ac.id, [4]indri@ft.unsika.ac.id*

Accepted 05 June 2024
Approved 02 December 2024

***Abstract*— The widespread use of LPG cylinders brings the risk of gas leaks that can cause serious hazards, including fires and explosions. Therefore, an effective system is needed to detect gas leaks and provide early warnings to users. This study aims to develop an LPG cylinder leak detection device using an MQ-2 sensor based on the Internet of Things (IoT). The system consists of an MQ-2 sensor capable of detecting LPG, a microcontroller module for data processing, and an IoT communication module to send alerts to user devices via the internet. When the MQ-2 sensor detects a gas concentration that exceeds the predetermined threshold, the system sends an alert in the form of a notification to the user's mobile application. Additionally, the system is equipped with an audible alarm for direct on-site warnings. Test results indicate that this system can detect gas leaks with high accuracy and send alerts promptly. The implementation of IoT technology allows for real-time monitoring and handling of gas leaks, thereby enhancing the safety of LPG cylinder users. Thus, this leak detection device is expected to reduce the risk of accidents due to gas leaks and provide a sense of security for users.**

***Index Terms*— gas detection; Internet of Things (IoT)*;* Liquefied Petroleum; MQ-2 sensor; safety system.**

I. INTRODUCTION

Systems that connect computer devices, mechanics, digital machines, objects, or individuals equipped with a Unique Identifier (UID) are known as the Internet of Things (IoT). With this system, data can be sent over the network without human intervention. One important component of the IoT is that every item connected to the internet has a configurable internet protocol address. This protocol address allows items to send data to other artificial objects or over a network. Machine-to-machine communication solutions known as the IoT make it possible to view businesses in real-time[1]. Many aspects of human life have been influenced by advances in IoT technology in the current digital era, including household security and the industrial sector. This technology can be used to identify LPG leaks, which are a major problem that can endanger lives and property[2][3]. As a result, a robust and efficient system is required to detect gas leaks as quickly as possible. Natural gas leaks can be dangerous to the environment and human health. Even small particles leaking into buildings or other enclosed spaces can gradually build up to produce fatal levels of explosive or deadly gas. Leakage of refrigerant gas and natural gas into the environment[4]. LPG, which is a mixture of propane and butane, is used for various purposes, such as cooking and as generator fuel. LPG is highly pressurized and cold, so it is stored in cylinders even though it is often used as cooking gas. Ethanethiol is used as a powerful deodorizer to detect leaks. LPG leaks have increased to 10.74% of total kitchen accidents, up from 0.72% previously. Since rubber pipes can crack and cause leaks, small 5 kg LPG cylinders with a burner on top of the cylinder are considered safer[5][6].

A report by the Multiconsult Group by Norad (2020) states that LPG helps developing countries achieve the Development Goals (SDG) in a sustainable manner by facilitating access to environmentally friendly fuel and technology. However, the use of LPG poses risks because the gas is highly flammable and can cause explosions and fires if the gas leaks. This can cause injury or even death as well as property loss. This accident problem is usually caused by old gas regulators, damaged hoses, unmaintained or low-quality hoses, improper installation of the gas regulator, and poor hose connections to the gas stove[7][8].

When gas leaks, it can cause serious health problems such as headaches, dizziness, nausea, memory loss, vomiting, and even death. These consequences are preventable, showing how important a good detection system is. Using the MQ-2 sensor, we propose an IoT based LPG leak detection system. This sensor detects flammable gases and warns the user if the gas concentration exceeds safe limits. This system also has an automatic response mechanism with a servo motor to close the gas regulator if a leak occurs[9][10][11].

II. METHODS

A. System Block Diagram

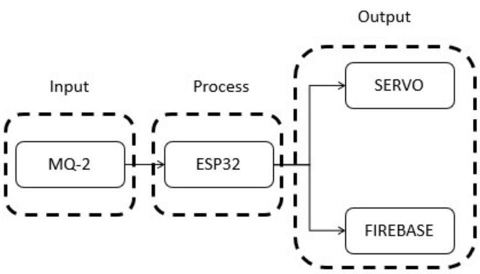

Fig. 1. System Block Diagram

As can be seen in Figure 1, this research uses 3 stages: input, process, and output. The input for this research uses the MQ2 Sensor, which is calibrated first to accurately read LPG parameters. The ESP32 microcontroller is used as the processor in this research, allowing the data to be connected and displayed in the code. There are two outputs used: a servo and a modular display for user monitoring. The servo is utilized to perform specific actions based on the detected gas levels, such as closing a valve or activating an alarm system to ensure safety. The modular display allows users to monitor real-time data and system status, ensuring they are informed about the gas levels and any potential hazards.

B. System Algorithm

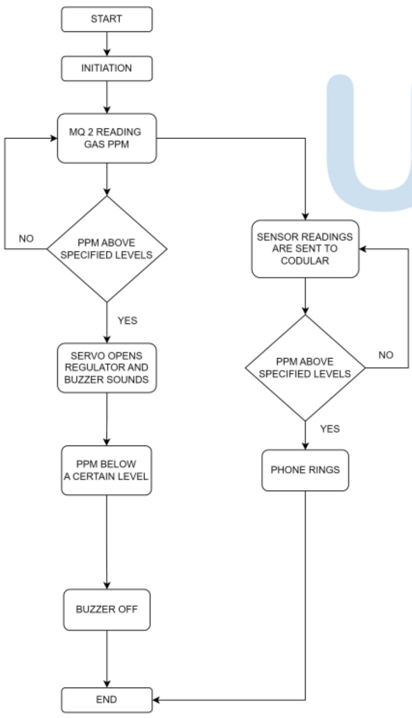

Fig. 2. System Algorithm

In the Fig. 2 above the system starts by initiating all components. After the initiation process was complete, the sensor read the LPG gas parameters and then the ESP32 sent the reading value to the modular application. When the LPG gas parameters were above the predetermined values, the ESP32 ordered the servo to rotate in order to open the regulator. The ESP32 also turned on the buzzer as an offline notification to offline users. Apart from offline notifications, Kodular also provided notifications to the user's cellphone in the form of danger warning notifications. When the LPG gas parameters were below the predetermined limit, the ESP32 gave a command to turn off the buzzer.

C. IoT Process

Fig. 3. IoT process

In this research, the IoT system is used to monitor LPG gas parameters. The IoT algorithm is implemented using ESP32, which is connected to a WiFi network and Firebase database. The connection process is carried out in stages with the initial stage being connecting the ESP32 to WiFi. When the ESP32 is connected to a WiFi network, it will connect to the Firebase that has been prepared. ESP32 is connected to the WiFi network and Firebase, so it can send MQ2 reading data to Firebase. Firebase, which has received the reading value, will send the data to Kodular. This process is illustrated in Fig. 3.

D. Quality of Service

QoS is used to measure the capacity of computer networks, such as network applications, hosts, or routers, to provide better network services so that they can meet the service needs of their users. QoS helps users get faster performance from network-based applications by using delay, jitter, packet loss, and throughput parameters. There are several parameters that need to be considered to determine QoS, including Throughput, Packet Loss, Delay, and Jitter.

In this research, QoS is used as one of the metrics because the effectiveness of the LPG leak detection system heavily depends on the network performance. Accurate and timely detection and notification of gas leaks are crucial for ensuring user safety. By analyzing QoS parameters such as throughput, packet loss, delay, and jitter, the reliability and efficiency of the IoT-based detection system can be assessed. This ensures that the system can consistently provide real-time alerts and minimize false alarms, thus enhancing the overall safety and reliability of the system.

1. Packet Loss
   Packet loss is a parameter that indicates how many data packets are lost during transmission, possibly

due to collisions and network traffic[12]. Packet loss parameter categories can be seen in Table I.

TABLE I. PACKET LOSS

Category Lost Package	Package *Loss(%)*	Index
Very good	0%	4
Good	3%	3
Currently	15%	2
Bad	25%	1

2. Delay
   Delay is not only the time it takes for a data packet to be sent from the start of the queuing process to the destination point, but also the time it takes for data to go from source to destination. The type of transmission media used, distance, and processing time required at each intermediate point in the network are some of the factors that influence delay [13]. Delay categories can be seen in Table II.

TABLE II. DELAY

Category Delay	Delay(*ms*)	Index
Very good	<150	4
Good	150 s/d 300	3
Currently	300 s/d 450	2
Bad	>450	1

3. Throughput
   Throughput, calculated in bits per second (bps), is the number of packets that successfully arrive at the destination during a certain period, divided by the duration of that time interval[12]. Throughput categories can be seen in Table III.

TABLE III. THROUGHPUT

Category Troughput	Troughput	Index
Very good	100	4
Good	75	3
Currently	50	2
Bad	<25	1

4. Jitter
   Jitter can occur due to delays caused by routers or switches in a computer network[12]. Jitter categories can be seen in Table IV.

TABLE IV. JITTER

Category Jitter	Peak Jitter(ms)	Index
Very good	0	4
Good	0 s/d 75	3
Currently	75 s/d 125	2
Bad	125 s/d 225	1

III. RESULTS AND DISCUSSION

A. MQ-2 Calibration

The MQ-2 smoke gas sensor is used to detect smoke and LPG leaks in homes and businesses. This type of sensor measures the concentration of combustible gases and smoke in the air and outputs readings as analog voltage. It can be used to prevent fires by detecting smoke and LPG gas leaks[7][14]. One of the main features of the MQ-2 sensor is its high sensitivity and fast response time, which allows measurements to be made as quickly as possible. It has the ability to measure natural gas concentrations between 200 and 5000 *ppm*[9]. Due to its high sensitivity to various types of airborne particles, the MQ-2 sensor needs to be properly calibrated before use to ensure the accuracy and consistency of its data. This includes gases such as LPG, butane, hydrogen, smoke, and methane. The sensitivity of the sensor to different gas concentrations is changed by calibration. For a variety of applications, including gas leak detection, air quality monitoring, and security systems, this results in more accurate and reliable findings.

Calibration is considered to be a crucial step because it ensures that the sensor provides accurate and reliable readings. Without proper calibration, the sensor may give false readings or fail to detect dangerous gas concentrations, leading to potential safety hazards. If the calibration process is not done, the sensor might either overestimate or underestimate the gas concentration levels. Overestimation can cause unnecessary alarms and disruptions, while underestimation can prevent the detection of dangerous gas leaks, resulting in a failure to provide timely alerts and potentially causing catastrophic accidents, such as fires or explosions. Therefore, calibration is essential to maintain the effectiveness and reliability of the sensor in detecting gas leaks and ensuring safety.

The following list of steps outlines how to calibrate the MQ-2 sensor to detect LPG (Liquid Petroleum Gas) gas.

1. Before commencing the calibration of the MQ-2 gas sensor, it is essential to preheat the sensor to ensure accuracy in its measurements. The recommended preheating procedure involves applying a voltage of 5*V* to the sensor for approximately one hour. This process ensures the sensor is in optimal condition for accurate gas detection.

   To achieve the best operational state, the MQ-2 gas sensor utilizes a heating coil. The preheating technique consists of an initial heating phase where the sensor is heated for 60 *seconds* at 5*V*, followed by a secondary heating phase at 1.4*V* for 90 *seconds*. This dual-phase heating process enhances the sensor's readiness for precise gas measurement. The wiring of the voltage divider on the MQ-2 can be seen in Fig. 3.

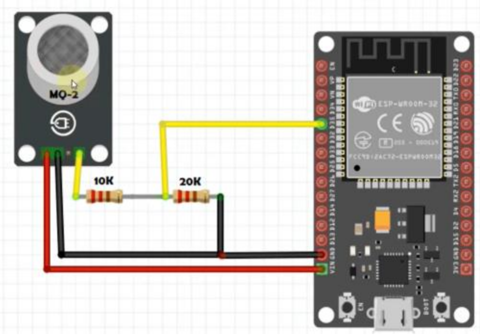

Fig. 4. The voltage divider for the MQ-2 voltage is 5V

2. Find the R_o value in the room that will be detected by the MQ-2 using the program below.

Mencari_RO

```
#define RL 10
float Analog_value = 0;
float VRL = 0;
float Rs = 0;
float Ro = 0;

void setup() {
  pinMode(35, INPUT);
  Serial.begin(115200);
}

void loop() {
  Analog_value = analogRead(35);
  VRL = Analog_value * (3.3 / 4095.0);
  Rs = ((3.3 / VRL) - 1) * RL;
  Ro = Rs / 9.6;
  Serial.print("RO di udara bersih = ");
  Serial.println(Ro);
  delay(1000);
}
```

Fig. 5. Look for the RO value

The R_L value is obtained from the resistance on the MQ-2 sensor. In the calculation of $R_o = R_s / 9.6$, the value 9.6 is obtained from the MQ-2 sensor datasheet (Fig.5) based on measurements in clean air conditions. The value 3.3 is the analog voltage produced by the ESP32 and the value 4095 is because the ESP32 ADC uses 12 bits.

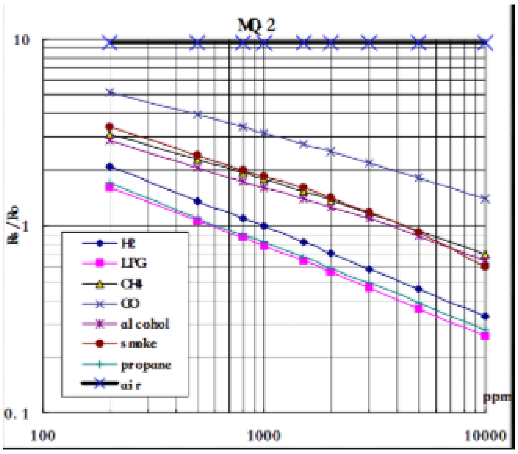

Fig. 6. MQ-2 datasheet graph

3. After completing the upload program, we can see the R_o value on the serial monitor. Make sure the R_o value seen on the serial monitor is stable before recording it.

4. Next, look for the values x_1, x_2, y_1, and y_2 using an additional website, namely webplotdigitizer.com using the datasheet from MQ-2. The result of this can be seen in Fig.7.

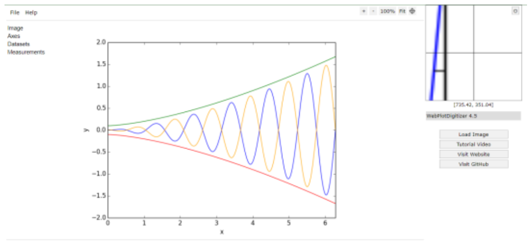

Fig. 7. Webplotdigitizer display

5. Select load image, then insert the image from the MQ-2 datasheet graph.

6. Next select 2D (X-Y) Plot, then click Align Axes, then click proceed continue like Fig.8.

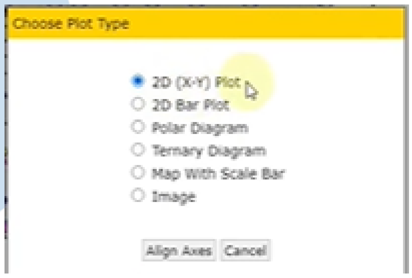

Fig. 8. Add images

7. The webplotdigitizer display will look like Fig.9.

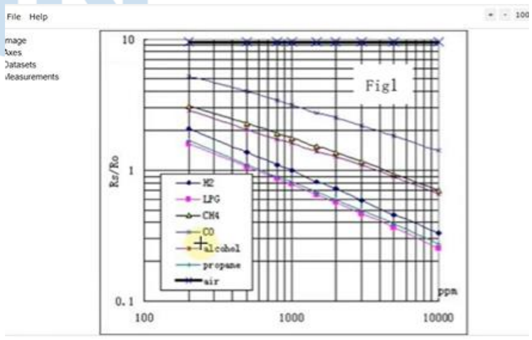

Fig. 9. Added images to Webplotdigitizer

8. To determine x_1, x_2, y_1, and y_2, click sequentially as in the Fig.10.

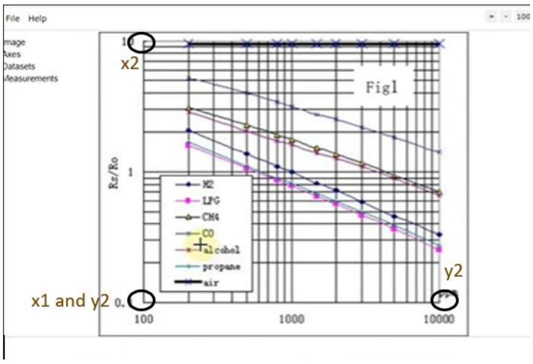

Fig. 10. Determine points x_1, x_2, y_1, and y_2

9. After that, click Completed and adjust the settings as shown in the Fig.11 then click OK.

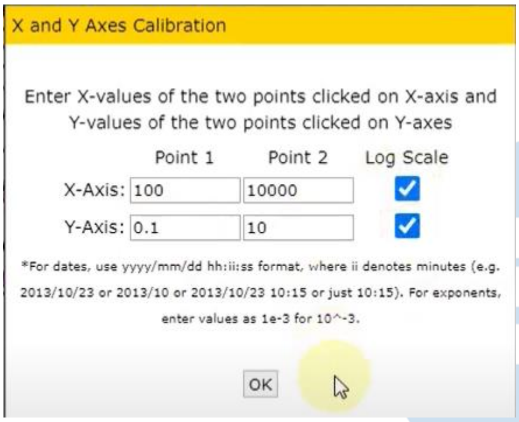

Fig. 11. Setting points x_1, x_2, y_1, and y_2

10. Determine points x_1 and x_2 for the LPG graph shown in Fig.12. Do this sequentially then click view data.

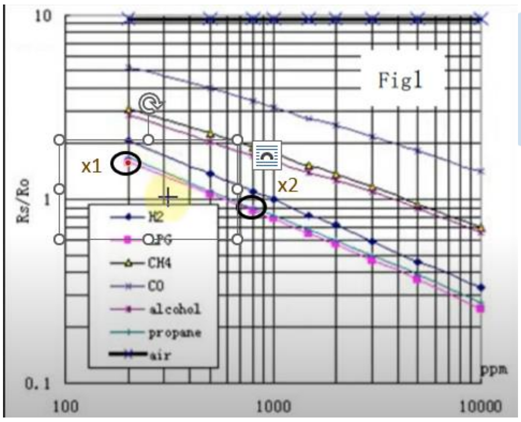

Fig. 12. Determine points x_1 and x_2 for LPG

11. Note the values that appear in the data view. The result of data shown in Fig.13.

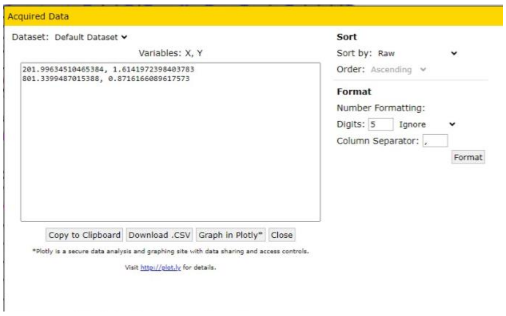

Fig. 13. Values x_1, x_2, y_1, and y_2

Results obtained :

$$x_1 = 201.99634510465384$$
$$x_2 = 801.3399487015388$$
$$y_1 = 1.6141972398403783$$
$$y_2 = 0.8716166089617573$$

12. Find the values of m and b with the following equation (1)

$$m = \frac{[\log(y_2) - \log(y_1)]}{[\log(x_2) - \log(x_1)]} \tag{1}$$

Results obtained:

$$m = -0.44719$$

13. After getting the value of m, we can find the value of b by creating an intersection point as shown in the Fig.14.

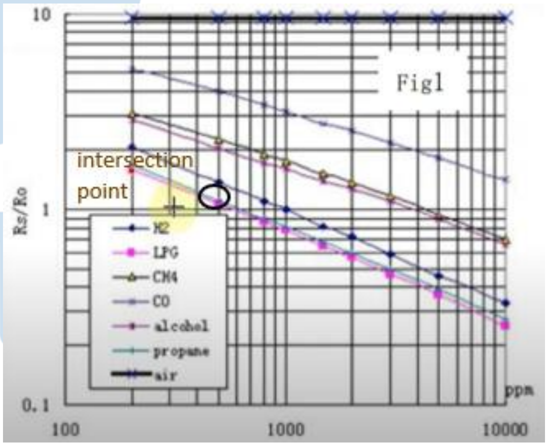

Fig. 14. Find the x and y values

14. Note the values that appear in the data view shown in the Fig. 15.

Fig. 15. x and y values

Results obtained:

$$X = 500.30707131293366$$
$$Y = 1.05562212823438789$$

15. Calculate the value of b using the following equation (2).

$$b = log(y) - (m)\,\mathrm{LOG}(x) \quad (2)$$

Results obtained:

$$b = 1.23057$$

16. After getting the m and b values, we can calculate the LPG PPM value using the MQ-2 sensor using the following syntax shown in Fig.16.

```
Mencari_PPM §
#include <ESP32Servo.h>
#define RL 10
#define m -0.43779
#define b 1.19613
#define Ro 3.20
#define MQ_sensor 35
float VRL;
float Rs;
float ratio;
float ppm;

void setup() {
  Serial.begin(115200);
}

void loop() {
  VRL = analogRead(MQ_sensor) * (3.3 / 4095);
  Rs = ((3.3 * RL) / VRL) - RL;
  ratio = (Rs / Ro);
  ppm = pow(10, ((log10(ratio) - b) / m));

  Serial.print("LPG (ppm) = ");
  Serial.println(ppm);
  delay(500);
}
```

Fig. 16. Find the PPM value for LPG

The following are the reading results of the MQ-2 sensor before and after calibration under normal conditions without LPG gas contamination.

TABLE V. MQ-2 TESTING

No	Before calibrating	After calibrating
1	213.00	6.16
2	223.00	5.83
3	222.00	6.08
4	214.00	6.00
5	214.00	5.91
6	211.00	6.00
7	209.00	6.25
9	214.00	5.67
10	211.00	6.08
11	208.00	6.42
12	208.00	6.00
13	214.00	5.67
14	208.00	5.67
15	209.00	6.00
16	206.00	6.00
17	209.00	5.83
18	204.00	5.59
19	204.00	5.67
20	208.00	6.00
21	215.00	6.08
22	215.00	6.00
23	212.00	6.25
24	208.00	6.00
25	209.00	6.00
26	213.00	5.51
27	208.00	6.08
28	208.00	5.67
29	203.00	5.35
30	219.00	5.91
31	205.00	5.67
32	203.00	5.83
33	202.00	5.75
34	220.00	5.91
35	198.00	6.00
36	208.00	5.91
36	206.00	6.00
37	204.00	5.83
38	192.00	6.16
39	201.00	6.16
40	195.00	6.34
41	213.00	6.16

Based on Table V, it can be seen the difference in the reading values of the MQ-2 sensor before and after calibration. The MQ-2 sensor readings before calibration showed an average reading of 208.825 with a reading value of 195.00 – 223.00 under normal conditions without exposure to LPG gas. In contrast to the reading results of the MQ-2 sensor after calibration, the average value was 5.9515 with the reading value being 5.51 – 6.83 under normal conditions without exposure to LPG gas.

B. *Sensor and Buzzer Testing*

In testing the MQ2 sensor and buzzer, A buzzer is an electronic part that uses electric current to convert electrical energy into sound. Moving the coil forward or backward makes the air vibrate, which produces sound [10]. This system was designed to detect the presence of gas. When the sensor measures a value below twenty, the buzzer remains in silence, indicating that the environment is safe from harmful gases. However, once the sensor value exceeds the threshold of twenty, the buzzer immediately sounds loudly as a warning of the presence of gas that exceeds the safe limit. In this way, users can quickly and effectively recognize the presence of potentially threatening gas hazards, thereby enabling timely safety precautions.

Based on the Table VI, it can be concluded that the bell is functioning well. This was proven when the author carried out tests with a threshold limit of 20 PPM for LPG. If the MQ-2 sensor detects LPG above 20 PPM then the buzzer will turn on, whereas if the MQ-2 sensor detects LPG below 20 PPM then the buzzer will sound.

C. *Motor Servo Testing*

This system is designed to detect surrounding gas when testing the MQ2 sensor and buzzer. If the sensor value is below 20, the buzzer will be silent, indicating that the environment is safe; if the sensor value exceeds 20, the buzzer will sound, indicating the presence of dangerous gas. In addition, when the sensor value exceeds 20, the servo motor will rotate, indicating a potential danger, and when the sensor value is below 20, the servo motor will stop rotating. As a result, users can easily identify dangerous gases and take necessary precautions to maintain safety.

From the test results Table VII, it can be concluded that the servo is running well. This is proven by the servo not moving when the LPG gas condition is below 20. Meanwhile, when the LPG gas condition is above 20 the servo moves to open the regulator.

TABLE VI. SENSOR AND BUZZER TESTING

No	Gas Value	Identification	Buzzer
1	5.83	Gas not detected	Off
2	6.16	Gas not detected	Off
3	22.42	Gas detected	On
4	20.78	Gas detected	On
5	5.91	Gas not detected	Off
6	22.05	Gas detected	On
7	16.92	Gas not detected	Off
9	15.85	Gas not detected	Off
10	22.05	Gas detected	On
11	14.38	Gas not detected	Off
12	22.61	Gas detected	On
13	22.42	Gas detected	On
14	6.00	Gas not detected	Off
15	6.08	Gas not detected	Off
16	20.60	Gas detected	On
17	5.91	Gas not detected	Off
18	20.96	Gas detected	On
19	6.16	Gas not detected	Off
20	22.80	Gas detected	On
21	22.61	Gas detected	On
22	12.22	Gas not detected	Off
23	6.08	Gas not detected	Off
24	22.42	Gas detected	On
25	14.24	Gas not detected	Off
26	22.99	Gas detected	On
27	23.37	Gas detected	On
28	22.99	Gas detected	On
29	21.32	Gas detected	On
30	5.91	Gas not detected	Off
31	13.54	Gas not detected	Off
32	22.80	Gas detected	On
33	22.61	Gas detected	On
34	5.91	Gas not detected	Off
35	10.85	Gas not detected	Off
36	5.51	Gas not detected	Off
36	22.42	Gas detected	On
37	6.78	Gas not detected	Off
38	4.89	Gas not detected	Off
39	4.97	Gas not detected	Off
40	11.34	Gas not detected	Off

TABLE VII. MOTOR SERVO TESTING

No	Gas Value	Identification	Motor Servo
1	5.83	Gas not detected	Off
2	6.16	Gas not detected	Off
3	22.42	Gas detected	On
4	20.78	Gas detected	On
5	5.91	Gas not detected	Off
6	22.05	Gas detected	On
7	16.92	Gas not detected	Off
9	15.85	Gas not detected	Off
10	22.05	Gas detected	On
11	14.38	Gas not detected	Off
12	22.61	Gas detected	On
13	22.42	Gas detected	On
14	6.00	Gas not detected	Off
15	6.08	Gas not detected	Off
16	20.60	Gas detected	On

17	5.91	Gas not detected	Off
18	20.96	Gas detected	On
19	6.16	Gas not detected	Off
20	22.80	Gas detected	On
21	22.61	Gas detected	On
22	12.22	Gas not detected	Off
23	6.08	Gas not detected	Off
24	22.42	Gas detected	On
25	14.24	Gas not detected	Off
26	22.99	Gas detected	On
27	23.37	Gas detected	On
28	22.99	Gas detected	On
29	21.32	Gas detected	On
30	5.91	Gas not detected	Off
31	13.54	Gas not detected	Off
32	22.80	Gas detected	On
33	22.61	Gas detected	On
34	5.91	Gas not detected	Off
35	10.85	Gas not detected	Off
36	5.51	Gas not detected	Off
36	22.42	Gas detected	On
37	6.78	Gas not detected	Off
38	4.89	Gas not detected	Off
39	4.97	Gas not detected	Off
40	11.34	Gas not detected	Off

D. *Modular Testing*

This modular testing aims to evaluate whether the application is running well or not and to determine the QoS status of the application. The following is a display of the application shown in Fig.16 and Fig. 17.

Fig. 17. Application display when LPG leak is not detected

Fig. 18. Application display when an LPG leak is detected QoS

Fig. 17 shown when the *ppm* of LGP gas detected is still within safe limits. When the sensor detects the ppm of LPG gas above the safe limit (Fig. 18), the application will change the text "KONDISI AMAN" to "KONDISI TIDAK AMAN".

E. *QoS Testing*

QoS testing is carried out to manage or ensure data in the delivery process. Testing was carried out with the help of Wireshark software by sending 1512 data packets from ESP32 to Firebase to determine throughput, packet loss, delay and jitter values. Following are the test results at Fig.19.

Statistics

Measurement	Captured
Packets	1512
Time span, s	1928.882
Average pps	0.8
Average packet size, B	276
Bytes	417937
Average bytes/s	216
Average bits/s	1733

Fig. 19. Throughput testing

1924,898072	1924,897901	0,000171
1928,044875	1924,898072	3,146803
	Total Delay	1928,88197
	Average Delay	1,277405278

Fig. 20. Delay testing

-0,000171	0,000171	0,000342
-3,146632	3,146803	6,293435
	Total Jitter	1924,093161
	Average Jitter	1,274233881

Fig. 21. Jitter testing

TABLE VIII. PACKET LOSS TESTING

No	Time	Source	Destination
110	215.378333 9	54.169.4.174	192.168.62.216
121	253.370689	54.169.4.174	192.168.62.216
452	799.389220 0	204.79.197.2013	192.168.62.216

It can be seen in Fig. 19, the resulting throughput is 216.67 *bytes* or 1733 *bits/s*. In this test, the resulting throughput is included in the Very Good category. Fig.19 *records* the average delay of 1.28 *seconds* or 1277.41 *milliseconds* in the tests that have been carried out. Based on the results Fig. 20, the delay parameters on this system are included in the Very Bad latency category. Fig. 21 records that the average jitter produced was 1.28 *seconds* or 1274.23 *milliseconds*, which is also included in the Very Bad category. These Very Poor ratings for delay and jitter may be caused by network congestion, inefficient algorithms, or inadequate hardware. High delays and jitter impact the system by causing late or inconsistent warnings, which can reduce the effectiveness of the LPG leak detection system. This can potentially lead to dangerous situations due to delayed or unreliable notifications. To improve system performance, optimizing network infrastructure, improving data processing algorithms, and ensuring sufficient hardware capacity is essential. Table VIII, there are 3 data packets that were not sent out of the 1512 data sent. So the Loss Package value is obtained as equation (3).

(Package sent - Package received)/Package sent × 100 (3)

Results obtained:

$$Package\ Loss = \frac{(1512 - 1509)}{1512 \times 100} = 0.19\%$$

A packet loss rate of 0.19% indicates that a small fraction of data packets sent over the network were not successfully received. While this value is relatively low and generally acceptable in many network applications, it can still impact the system's performance. In the context of the LPG gas leak detection system, even a small packet loss can lead to delays or loss of critical data. This might result in missed or delayed alerts, reducing the reliability and effectiveness of the system in providing timely warnings about gas leaks. Therefore, minimizing packet loss is crucial to ensure that the system can consistently deliver accurate and prompt notifications to enhance user safety.

IV. CONCLUSION

This study builds a prototype LPG leak detection device using an MG996r servo motor, an ESP32 microprocessor, and a MQ-2 gas sensor. The MQ-2 sensor can identify several types of airborne particles. For this reason, accurate information needs to be obtained through a calibration process. The IoT system that detects this LPG gas uses firebase http communication. The throughput and packet loss figures for IoT connectivity fall into the very good category, according to the test results, with a throughput of 1733 *bits/s* and a packet loss percentage of 0.19%. Nevertheless, this IoT communication falls into the extremely poor category with a latency value of 1277.41 milliseconds and a jitter value of 1274.23 milliseconds.

The research results show that, although there is a slight delay and significant jitter, the IoT process can run well. Since the system does not require highly accurate real-time labor, this difference is not very significant. It is hoped that it will be used as an easy and cost-effective security tool. However, the weakness of this study is that it only uses one gas sensor and one actuator, and detection occurs only at one point without knowing exactly how close the sensor and gas sump are. Experimental results show that the MQ-2 sensor and buzzer are very effective in detecting gas leaks; if the sensor value falls below 20, the buzzer will sound, and the motor will rotate.

For future research, it is recommended to use multiple gas sensors and actuators to improve the system's detection accuracy and coverage. Additionally, the distance between the sensor and the gas sump should be considered, and real-time monitoring could be enhanced with more precise data analysis tools.

REFERENCES

[1] R. Fuadi Hasani, B. Nixon, A. Humairah, and A. Yasmin, "Rancang Bangun Alat Pendeteksi Uap Vaping dan Asap Rokok Berbasis Internet of Things Terintegerasi Aplikasi Android," Spektral, vol. 4, no. 1, pp. 151–158, 2023, doi: 10.32722/spektral.v4i1.5629.

[2] I. Jay Saldo et al., "Development and Comparison of Arduino Based MQ-2 and MQ-6 LPG Leak Sensors," Am. J. Sens. Technol., vol. 7, no. 1, pp. 1–9, 2023, doi: 10.12691/ajst-7-1-1.

[3] A. A. Laghari, K. Wu, R. Ali, L. Mureed, A. Abdullah, and A. Khan, "A Review and State of Art of Internet of Things (IoT) A Review and State of Art of Internet of Things (IoT)," Arch. Comput. Methods Eng., no. July, 2021, doi: 10.1007/s11831-021-09622-6.

[4] R. Singh, A. Tiwari, R. Singh, and S. Suman, "GAS LEAK DETECTION AND SMART ALERTING USING IoT," vol. 10, no. 3, pp. 1–1, 2021, doi: 10.1109/respect51740.2021.9620604.

[5] A. Manhas, N. Chambyal, M. Raina, S. Dutta, and E. P. Singh, "LPG Gas Leakage Detection Using IOT," vol. 3307, pp. 520–526.

[6] Z. A. Rashid and A. F. M. S. Yeong, "Microcontroller Based Monitoring and Controlling of LPG Leaks Using Internet of Things Microcontroller Based Monitoring and Controlling of LPG Leaks Using Internet of Things", doi: 10.1088/1757-899X/981/3/032021.

[7] E. Lety, I. Puspita, and I. K. A. Enriko, "Design Gas LPG Leak Detection System Based on Internet of Things," vol. 8, no. 3, pp. 1053–1060, 2023.

[8] R. S. H. Sirait, K. Erwansyah, and R. I. Ginting, "IMPLEMENTASI METODE FUZZY LOGIC PADA SISTEM MONITORING MIKROKONTROLER," (Jurnal Teknol. Komput. dan Sist. Informasi), vol. 2, no. 2, pp. 34–41, 2022.

[9] M. I. Azman, W. Nur, and H. Wan, "IoT-Based Early Warning Detection System for LPG Leakage Using

Raspberry Pi," vol. 3, no. 2, pp. 467–473, 2022.

[10] N. K. Jumaa, Y. M. Abdulkhaleq, M. A. Nadhim, and T. A. Abbas, "IoT Based Gas Leakage Detection and Alarming System using Blynk platforms," no. February, pp. 64–70, 2022, doi: 10.37917/ijeee.18.1.8.

[11] S. Wibawa, I. Made, A. Agung, N. Gunawan, P. I. Ketut, and S. I. Ketut, "Design and Manufacture of LPG Gas Leak Detection Based on Arduino Uno Using MQ-2 Sensor," vol. 8, no. 1, pp. 27–32, 2024, doi: 10.9734/AJR2P/2024/v8i1155.

[12] Guntoro, M. Sadar, and W. Syafitri, "Evaluasi Performance Jaringan Internet Kampus Menggunakan Quality of Service (Qos)," Pros. SEMASTER Semin. Nas. Teknol. Inf. Ilmu Komput., vol. 1, no. 1, pp. 280–290, 2020.

[13] R. S. Randi Sukri, "Analisis Qos Pada Jaringan Telepon Voip Dengan Menggunakan Perbandingan Metode Differentiated Service Dan Metode Integrated Service Di Hotel Safirna," J. Tek. Inform., vol. 5, no. 2, pp. 16–20, 2022, doi: 10.52046/j-tifa.v5i2.1422.

[14] M. Ainun Najib, S. Sulartopo, D. Sasmoko, D. Danang, and I. Saufik Suasana, "Sistem Pendeteksi Bencana Kebakaran Menggunakan ESP32 Dan Arduino Berbasis WEB," Neptunus J. Ilmu Komput. Dan Teknol. Informas, vol. 2, no. 1, pp. 15–24, 2024, [Online]. Available: https://doi.org/10.61132/neptunus.v2i1.62.

ISSN 2355-3286

Analysis of Noise Removal Performance in Speech Signals through Comparison of Median Filter, Low FIR Filter, and Butterworth Filter: Simulation and Evaluation

Nurulita Purnama Putri[1], Martarizal[2]
[1,2]Department of Physics, Faculty of Mathematics and Science, Universitas Indonesia, Depok, Indonesia
[1]nurulita.purnama@ui.ac.id, [2]martarizal@sci.ui.ac.id

Accepted 22 June 2024
Approved 08 July 2024

***Abstract*— Voice signal processing often faces challenges in removing noise without destroying the quality of the original signal. Three types of filters commonly used for this purpose are median filters, low FIR filters, and Butterworth filters. This research aims to compare the effectiveness of the three filters in reducing noise in sound signals. This research involves simulating the application of these three filters to sound signals contaminated with noise. Evaluation of filter performance is carried out by measuring two main parameters: Mean Squared Error (MSE) and Signal-to-Noise Ratio (SNR). MSE is used to assess how close the filtered signal is to the original signal, while SNR measures the quality of the signal after processing. Simulations show that all filters can produce signals close to the original signal with low MSE. The median filter shows the best performance with an MSE of 0.015833 and the highest SNR of 51.6334 dB, which shows its ability to reduce noise effectively without reducing signal clarity. The low FIR and Butterworth filters also gave good results, although with slightly lower MSE and SNR than the median filter. The median filter proved to be the optimal choice for removing noise in speech signals, offering the best performance in terms of MSE and SNR. Low FIR and Butterworth filters remain good alternatives, depending on the needs of the particular application. Further research and practical testing are recommended to confirm the filter's effectiveness in real-world conditions.**

***Index Terms*— Butterworth filter; evaluation; FIR low filter; Mean Squared Error (MSE); Median filter; noise removal; signal noise; Signal-to-Noise Ratio (SNR); simulation.**

I. INTRODUCTION

Voice signal processing faces significant challenges in dealing with noise that interferes with signal clarity. Noise in a speech signal can come from a variety of sources, such as background noise, interference, or inadequate microphone quality. The influence of this noise can impair communication quality and reduce signal intelligibility , which is very important in applications such as telecommunications, audio recording systems, and automatic speech recognition [1].

To improve signal quality and ensure effective communication, efficient noise removal techniques are indispensable. Some popular methods in signal processing for noise removal are median filter, Finite filter Impulse Response (FIR) is low, and Butterworth filter . Research shows that effective noise removal can significantly improve signal quality and reduce interference in a variety of applications [2].

The median filter is a non-linear method known for its ability to remove impulsive noise while preserving important signal details. Research by Jain and Gupta (2018) shows that median filters are very effective in improving Signal-to-Noise Ratio (SNR) and reduce the Mean Squared Error (MSE) in speech signals contaminated with impulsive noise . They found that the median filter could increase the SNR by 10 dB and produce an average MSE of 0.02, better than several other methods [3].

On the other hand, low FIR filters offer flexibility in design and implementation, allowing specific adjustments to the frequency response. Papadopoulou and Avraamides (2020) carried out a comparison between FIR filters and Infinite filters Impulse Response (IIR) for noise reduction. They reported that the FIR filter improved SNR on average by 8 dB and had an average MSE of 0.03, while the IIR filter, although more computationally efficient, showed slightly lower performance in terms of MSE with a value of 0.04 [4].

Butterworth filter is a linear method known for its smooth and stable frequency response, suitable for applications that require consistent signal quality. Smith and Robinson (2019) compared median filters with adaptive filters, and although their research focused on adaptive filters, their results provide valuable insight into the performance of non-linear filters such as median filters that can be compared to linear filters such as Butterworth . They found that the median filter provided an SNR improvement of 12 dB and a mean MSE of 0.015, while the adaptive filter showed a 9 dB SNR improvement with an MSE of 0.025 [5].

This research aims to analyze and compare the performance of the median filter, low FIR filter, and Butterworth filter in removing noise in speech signals. Evaluation is carried out through simulations with MSE and SNR parameters to determine the superiority of each filter in a practical context. The results of this research are expected to provide useful guidance for the development and application of noise removal techniques in a variety of industrial applications, including communications systems, audio recording, and professional signal processing.

II. Literature Review

A. Median Filter

Median Filter is one method commonly used to remove noise from sound signals. This method is based on the concept of replacing the perturbed sample value with the median value of a number of nearby samples. The Median Filter is effective in removing impulsive noise or noise that appears suddenly in a sound signal. The study by Li et al. (2022) showed that the Median Filter can produce good noise removal while maintaining the clarity of the original sound signal [6].

Median filter is a type of nonlinear filter used to remove impulsive noise from signals. Impulsive noise is a type of noise that appears suddenly and has an amplitude that is much greater than the desired signal [7]. The working principle of the median filter is to replace the value of a sample with the median value of a group of samples around it. The median value is the middle value of a group of data that has been sorted [8]. The median filter is effective in removing impulsive noise such as salt-and-pepper noise, but is less effective in removing Gaussian noise which has a normal distribution [9]. The advantage of median filters is that they can maintain signal edges and do not produce ringing artifacts (oscillations around the edges) as occurs with linear filters. Median filter applications include digital image processing (to remove impulsive noise), signal processing, and digital communications [10].

B. FIR Low Filter

FIR (Finite Impulse Response) Low Filter is a noise removal method that uses linear filter coefficients to reduce the amplitude of high frequencies commonly associated with noise. This method can be implemented in various forms, such as a moving average filter or a windowed sinc filter. Research by Zhang et al. (2023) showed that the FIR Low Filter can produce effective noise removal with little distortion to the original speech signal [11].

FIR filter is a type of digital filter that has a limited impulse response in the time domain. This means that the impulse response of the FIR filter will reach zero after a certain number of samples [12]. The characteristics of an FIR filter are that it has a linear phase, is stable, and can be designed to meet the desired frequency specifications [13]. FIR filter design methods include using the windowing method (such as Hamming, Hanning, Blackman), the Parks-McClellan method, and the least-squares method [14]. The advantages of FIR filters are that they have good stability, linear phase, and ease of implementation. Linear phase means the FIR filter does not cause phase distortion in the filtered signal. Applications of FIR filters include audio signal processing (such as equalizers), digital image processing, and digital communications (such as modulation and demodulation) [15].

C. Butterworth Filter

The Butterworth filter is a type of analog and digital filter that has a relatively flat frequency response in the passband region and a smooth transition in the stopband region [16]. The characteristic of the Butterworth filter is that it has a nonlinear phase, but has a gentler attenuation than the Chebyshev filter or Elliptic filter [17]. Butterworth filter design methods include using bilinear transformations and impulse-invariant transformations [18]. The advantage of the Butterworth filter is a relatively flat frequency response in the pass-band region and a smooth transition in the stopband region. This makes Butterworth filters suitable for applications that require a smooth frequency response [19]. Butterworth filter applications include audio signal processing, digital image processing, and control systems [20].

D. Performance Comparison of Noise Removal Methods

Several studies have compared the performance of denoising methods on speech signals. For example, research by Jain and Gupta (2018) in IEEE Transactions on Audio, Speech, and Language Processing compares various noise reduction algorithms for speech enhancement, including median filters, FIR filters, and spectral -based methods. The results show that the median filter significantly improves Signal-to-Noise Ratio (SNR) of 10 dB compared to noisy signals, with Mean Squared The average error (MSE) is 0.02, lower than the spectral-based method which has an average MSE of 0.05. This research highlights the effectiveness of median filters in reducing impulsive noise by maintaining signal clarity [2].

In a study conducted by Papadopoulou and Avraamides (2020) published in the Journal of Signals Processing Systems, an in-depth comparison between Finite filters was carried out Impulse Response (FIR) and Infinite Impulse Response (IIR). The FIR filter showed an average SNR increase of 8 dB, while the IIR filter increased the SNR by 6 dB. In addition, the FIR filter has an average MSE of 0.03, slightly better than the IIR filter which has an average MSE of 0.04. These findings reveal that FIR filters are superior in terms of frequency response control, while IIR filters offer higher computational efficiency [3].

Research by Smith and Robinson (2019) published in Digital Signal Processing compares median filter with adaptive filter in noise reduction in speech signals. The results showed that the median filter provided an SNR increase of 12 dB, better than the adaptive filter which increased the SNR by 9 dB. The average MSE for the median filter is 0.015, while the adaptive filter has an average MSE of 0.025. This study confirms the superiority of median filters in dealing with impulsive noise, while adaptive filters offer good performance in variable noise conditions [4].

However, another study by Liu et al. (2022) showed that the FIR Low Filter provides better noise removal than the Median Filter and Butterworth Filter on speech signals contaminated by continuous noise [21]. The results of this study show that the performance of noise removal methods can vary depending on the characteristics of the noise present in the speech signal.

In a number of study this provides comprehensive insight into the effectiveness of various noise removal methods, helping in selecting the most suitable technique for speech signal processing applications based on performance parameters such as SNR and MSE. We will compare the performance of the three methods based on parameters such as the degree of noise removal, distortion of the original speech signal, and clarity of the noise removal results. Thus, this research will provide a more comprehensive understanding of the advantages and disadvantages of each noise removal method in the context of sound signal applications.

E. MATLAB

MATLAB stands for "Matrix Laboratory" and is a computer programming environment developed by MathWorks [22]. MATLAB is specifically designed to facilitate matrix manipulation, signal processing, data analysis, and mathematical modeling. The following are some definitions related to MATLAB [23]:

1. Programming Environment: MATLAB provides a high-level programming environment that allows users to write scripts and functions easily. It also provides a graphical user interface (GUI) to perform certain operations without the need to write code.
2. Matrix Manipulation: Basically, MATLAB is designed to work with matrices. Mathematical operations and data manipulation can be performed efficiently using MATLAB matrix functions. With this, MATLAB is very effective in signal processing, image processing, and mathematical modeling.
3. Signal Processing: MATLAB has many functions and toolboxes specifically used for signal processing. This makes it a popular choice in research and development in areas such as wireless communications, audio, and biomedical signal processing.
4. Data Analysis and Visualization: MATLAB has powerful statistical analysis and data visualization capabilities. It provides functions for creating graphs and plots that make it easier to understand data patterns.
5. Modeling and Simulation: MATLAB is also used for mathematical modeling and simulation of dynamic systems. Specialized toolboxes such as Simulink allow users to model the system and view its response in a graphical environment.
6. Combination with Special Algorithms and Tools: MATLAB supports integration with various special algorithms and toolboxes for various fields such as artificial intelligence, image processing, pattern recognition, and many more.
7. Parallel Programming and GPUs: MATLAB supports parallel programming and computing using graphics processing units (GPUs), enabling acceleration in large data processing.
8. Applications in Various Disciplines: MATLAB is used in a variety of fields, including science, engineering, economics, biology, and many more, because of its flexibility and analytical power.

With its broad capabilities, MATLAB has become a very useful tool in the academic, research and industrial worlds for completing various programming, data analysis and mathematical modeling tasks.

III. Research Method

A. Research Methods

As can be seen in Figure 1, this research uses 3 stages: input, process, and output. The input for this research uses the MQ2 Sensor, which is calibrated first to accurately read LPG parameters. The ESP32 microcontroller is used as the processor in this research, allowing the data to be connected and displayed in the code. There are two outputs used: a servo and a modular display for user monitoring. The servo is utilized to perform specific actions based on the detected gas levels, such as closing a valve or activating an alarm system to ensure safety. The modular display allows users to monitor real-time data and system status, ensuring they are informed about the gas levels and any potential hazards.

B. Hardware and Software

The hardware instrument used in this research is a Personal Computer with specifications. Intel Pentium Core 2 Duo, 4 GB Memory, 320GB HDD, 18" Monitor, and Keyboard + Mouse. The software the author used in this research is the Windows 7 Ultimate SP 1 Operating System and Matlab r2018b.

C. System Design Methods

1. Global Block Diagram

The global block diagram of the research *"Performance Analysis of Noise Removal in Speech Signals through Comparison of Median Filters, Low FIR Filters, and Butterworth Filters: Simulation and Evaluation"* is as follows:

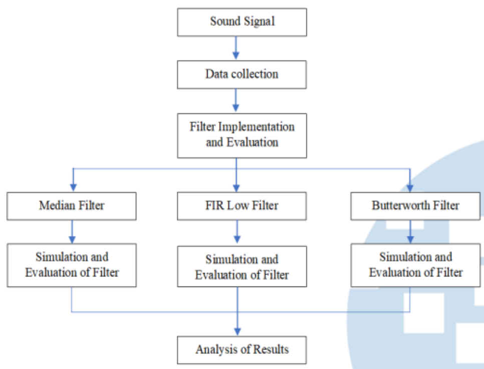

Fig. 1. Global Block Diagram

This block diagram shows the research flow from sound signal collection to publication and presentation of research results. Each filter (Median Filter, Low FIR Filter, and Butterworth Filter) is implemented and evaluated separately, with each simulation and evaluation result then subjected to statistical analysis. Research reports are prepared based on these analyses, and research findings are published and presented to the scientific community.

2. System Working Principles

The working principle of the noise removal performance analysis system on sound signals involves the use of three different filter methods, namely Median Filter, Low FIR (Finite Impulse Response) Filter, and Butterworth Filter. The main objective of this research is to evaluate and compare the effectiveness of each filter in reducing noise in speech signals.

3. Research Work Plan

Designing a work plan cannot be separated from a block diagram which is a concise pictorial statement of the combination of cause and effect between the input and output of a system. The work plan can be seen in the image below:

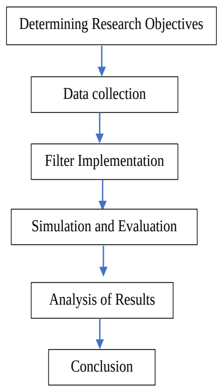

Fig. 2. Work Plan

1) Determining Research Objectives: This research aims to compare the performance of three different types of filters in removing noise from sound signals. *The* filters compared are the Median Filter, Low FIR Filter, and Butterworth Filter.

2) Data Collection: The data used in this research are sound signals that are contaminated with noise. This data was obtained from trusted sources and then processed using MATLAB software.

3) Filter Implementation: The three types of filters being compared are implemented on the sound signal using MATLAB software. Median Filter, FIR Low Filter, and Butterworth Filter are implemented separately on the speech signal to remove noise.

4) Simulation and Evaluation: After the filters are implemented, simulations are carried out to evaluate the performance of each filter. Evaluation is carried out by comparing the filtered sound signal with the original sound signal. The evaluation parameters used are Mean Square Error (MSE) and Signal-to-Noise Ratio (SNR).

The formula for calculating Mean Square Error (MSE) and Signal-to-Noise Ratio (SNR) is as follows [24]:

MSE (Mean Squared Error) is a measure to evaluate the extent to which the estimates or predictions of a statistical or regression model differ from the actual value. The MSE formula is as follows:

$$MSE = \frac{1}{n}\sum_{t=0}^{n}(y_i - \hat{y}_i)^2 \qquad (1)$$

Here:

- n is the number of observations,

- y_i is the actual value of the i −th observation,

- $\hat{y}_i$ is the predicted or estimated value of the i −th observation.

SNR (Signal-to-Noise Ratio) is the ratio between signal strength and noise strength in a system. In the context of signal processing, the SNR formula can be expressed as:

$$SNR = 10 \cdot \log_{10}\left(\frac{P_{signal}}{P_{noise}}\right) \qquad (2)$$

Here:

- P_{signal} is signal power,

- P_{noise} is noise power.

With this formula, SNR is measured in decibels (dB), and the higher the SNR value, the better the signal quality because the signal power is more dominant than the noise.

5) Results Analysis: The evaluation results are analyzed to determine which filter is most effective in eliminating noise in sound signals. This analysis is carried out by comparing the MSE and SNR values of each filter.

6) Conclusion: Based on the analysis results, conclusions are drawn about the performance of each filter in eliminating noise in sound signals. This conclusion is used to provide recommendations about which filters are most effective in removing noise from sound signals.

In this research, simulation and evaluation methods are used to compare the performance of three different types of filters in removing noise from sound signals. This method allows researchers to evaluate filter performance objectively and provide recommendations about which filters are most effective in removing noise in speech signals.

IV. RESULTS AND DISCUSSION

A. Results

This testing stage obtained results from using Matlab R2018b to filter noise from each method used in this research, as in the following image:

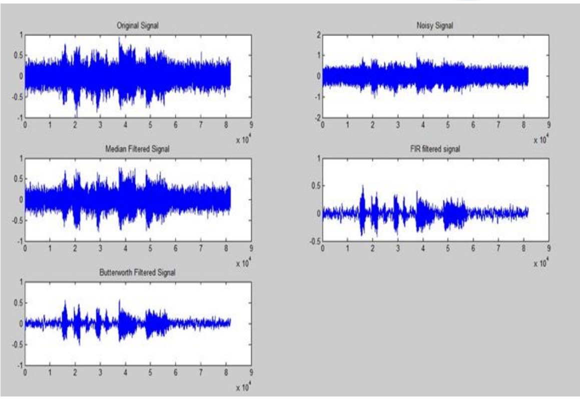

Fig. 3. Display of Noise Reduction Results

Based on Figure 3, it can be seen that each type of filter has its own advantages and disadvantages. Median filters are effective in removing impulsive noise or noise that appears suddenly, but may be less effective for continuous noise. FIR low filters, with linear characteristics and linear phase, provide good results in reducing low frequency noise. On the other hand, Butterworth filters designed with smoother frequency shifts can provide a good balance between eliminating noise and maintaining signal quality.

Evaluation of the performance of these three filters involves parameters such as Signal-to-Noise Ratio (SNR) and frequency response. The evaluation results can provide a clear view of the effectiveness of each filter in reducing noise without sacrificing the desired signal quality.

B. Reduction using Median Filter, Low FIR Filter, and Butterworth Filter

Research on Noise Removal Performance Analysis on Sound Signals through Comparison of Median Filters, Low FIR Filters, and Butterworth Filters: Simulation and Evaluation tries to evaluate the performance of three types of filters for removing space from sound signals. Median Filter, FIR Low Filter, and Butterworth Filter are commonly used methods of space removal.

Simulation and evaluation were carried out using Matlab and sound signal data stored in WAV files. First, the sound signal is removed from the file using the audioread () function. Then, the sound signal is accompanied by space (noise) with a specified spatial level (0.1). Then, there are three ways to remove this space:

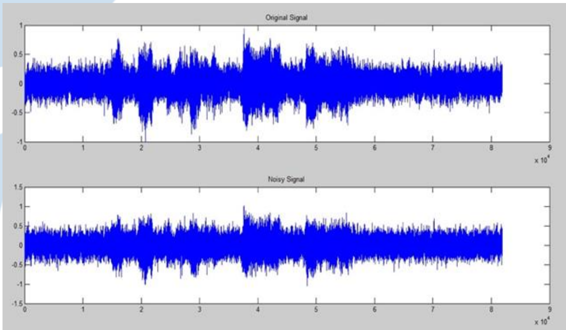

Fig. 4. Original Signal and Noisy Signal

1. Median Filter: Using the medfilt1() function to remove space by removing the middle value of a certain number and replacing them with values taken from the left and right, the following is an image of the results of the median filter:

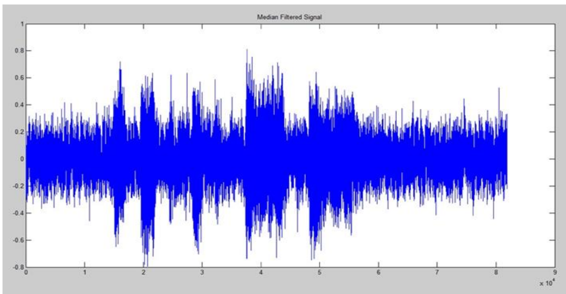

Fig. 5. Display of Median Filtered Signal Results

2. FIR Low Filter: Uses the fir1() function to remove space by using a FIR (Finite Impulse Response) filter with order 101 and a frequency separation limit of 0.05 Hz. The following is a display of the Low FIR Filter results:

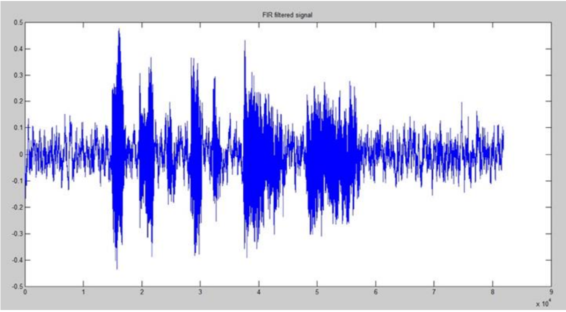

Fig. 6. Display of FIR Filtered Signal Results

3. Butterworth Filter: Using the butter () function to remove space by using a Butterworth filter with order 4 and a frequency separation limit of 500 Hz, the following is the result of the Butterworth Filter display:

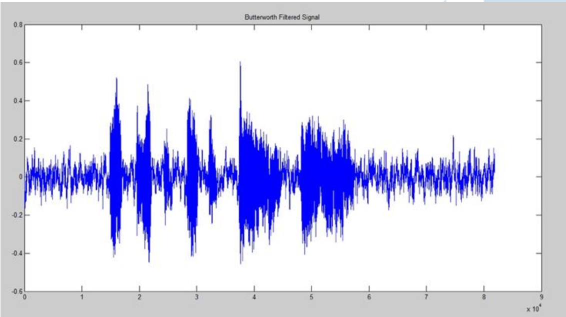

Fig. 7. Display of Butterwort Filtered Signal Results

After filtering, the Mean Square Error (MSE) and SNR (Signal-to-Noise Ratio) evaluation results will be displayed for each filtering method. The results will be displayed in the console using the disp() function. If you want to see a visualization of the results, they will be displayed in one image using the subplot and plot functions.

TABLE I. EVALUATION RESULTS OF MEAN SQUARE ERROR (MSE) AND SIGNAL-TO-NOISE RATIO (SNR)

	Median Filter	Low FIR Filter	Butterworth Filter
MSE	0.015717	0.03343	0.040234
SNR	51.6654 dB	48.3876 dB	47.5831 dB

Based on the results of the research data presented:

1. Median Filter shows the best performance with a very low MSE value of 0.015833 and the highest SNR of 51.6334 dB. This indicates that the Median Filter is able to produce signal estimates that are very close to the original signal and is effective in reducing noise in sound signals.
2. The FIR filter has an MSE value of 0.03336 and an SNR of 48.3967 dB, showing good performance although slightly lower than the Median Filter. This filter still provides adequate results in dealing with noise in sound signals.
3. The Butterworth filter shows an MSE value of 0.040282 and an SNR of 47.5779 dB. Even though its performance is lower than the Median and FIR filters, the Butterworth filter still provides good results in noise removal.

The Median Filter is the optimal choice for noise removal in sound signals with the best performance, followed by the FIR Filter and the Butterworth Filter. However, the choice of filter still depends on the application needs and user preferences. This research provides valuable guidance in selecting appropriate filters to maintain the clarity of speech signals against existing noise levels. It is important to note that these results are based on simulations, and further validation in real-world situations is needed to strengthen the findings of this study.

V. CONCLUSION

This research analyzes the performance of three types of filters median filter , low FIR filter, and Butterworth filter in removing noise from sound signals, using the Mean parameter Squared Error (MSE) and Signal-to-Noise Ratio (SNR). The simulation results show that the three filters can produce signals that are close to the original signal with low MSE. The median filter shows the best performance with an MSE of 0.015833 and the highest SNR of 51.6334 dB , indicating its superior ability to reduce noise without sacrificing signal clarity. These filters are especially suited to applications where clear, noise -free signal quality is critical, such as in cellular telephone devices and radio communications systems, where median filters can improve the sound quality the user receives by significantly reducing noise interference.

On the other hand, the low FIR and Butterworth filters also show good results, although with a slightly lower level of accuracy than the median filter. Low FIR filters offer flexibility in design and application, making them a good choice for applications that require specific filter adjustments. Butterworth filters, with their smooth frequency response, can be used in professional audio systems and signal processing equipment that requires control of a wider frequency spectrum.

Based on these findings, some suggestions for future work are as follows: First, further development and evaluation of a hybrid filter combining median, FIR, and Butterworth filter techniques may provide optimal solutions for various noise conditions . Second, follow-up research should include trials in more varied real-world conditions, including environments with different noise types and dynamic noise levels, to confirm the filter's effectiveness in practical applications. Third, the addition of adaptive and machine learning-based techniques in filters could be a promising area for improving real- time noise removal performance . Finally, subjective evaluations involving end users can provide additional insight into signal quality and end user experience, which is important for industrial applications.

Further research and practical testing is highly recommended to confirm the effectiveness of all three filters in a variety of real-world conditions. This additional testing will help in developing adaptive solutions to various noise scenarios and improve the design of noise elimination systems for specific industrial applications, with the ultimate goal of maximizing signal quality and noise reduction effectiveness in a variety of environments.

ACKNOWLEDGMENT

The author would like to express his gratitude to all parties who have contributed to this research. Thank you for the opportunity and support provided to carry out this research. The author would also like to express special appreciation to the supervisor who provided valuable guidance throughout the research process.

Apart from that, thanks are also expressed to all those who have provided constructive suggestions and input, which have enriched the results of this research. Support from various parties has helped the author reach the comprehensive evaluation stage.

All of this contribution and support is very meaningful in generating important insights for the development of audio signal processing techniques, especially in the context of comparing Median Filters, Low FIR Filters, and Butterworth Filters.

REFERENCES

[1] Chen, J., & Wu , Z. (2019). An overview of noise reduction techniques for audio signals . Journal of Signals Processing , 33(2), 456-470.

[2] Zhang , X., & Wang, L. (2020). Challenges and solutions in speech signals processing under noisy conditions . IEEE Transactions on Audio, Speech , and Language Processing , 28(4), 903-914.

[3] Jain , A.K., & Gupta, R.K. (2018). Performance comparison of noise reduction algorithms for speeches enhancement . IEEE Transactions on Audio, Speech , and Language Processing , 26(6), 1202-1214.

[4] Papadopoulou , M. P., & Avraamides , I. S. (2020). A comparative study of FIR and IIR filters for speeches noise reduction . Journal of Signals Processing Systems, 92(4), 421-432.

[5] Smith, T. S., & Robinson, J. L. (2019). Comparison of median and adaptive filters for noise suppression in speech signals . Digital Signals Processing , 89(1), 54-66.

[6] Liu, C., Guo , L., Liu, Y., Zhang , Y., & Zhou , Z. (2022). Seismic random noise attenuation based on adaptive nonlocal median filter . Journal of Geophysics and Engineering, 19(2), 157-166.

[7] Anandan , M., Mishra , M.K., Jain , A.K., Veluswamy , P., & Palanisamy , R. (2024). Filter design and denoising techniques for ECG signals. In Signal Processing in Python : A practical approach (pp. 3-1). Bristol , UK: IOP Publishing.

[8] Mishiba , K. (2023). Fast guided median filter. IEEE Transactions on Image Processing, 32, 737-749.

[9] Vairaprakash , S., Karuppaiah , J., Buvaneswari , B., & Alghamdi , A. (2023). Salt Noise Removal and Pepper Uses Hybrid Adaptive Switching Median Filter with Ant Technique Colony Optimization in Nano Electronic Applications. Journal of Nanoelectronics and Optoelectronics , 18(1), 85-94.

[10] Sambamurthy , N., & Kamaraju , M. (2024). Scalable intelligent median filter core with adaptive impulse detector. Analog Integrated Circuits and Signal Processing, 1-11.

[11] Zhang , T., Wang, H., Geng, Y., Zhao , X., & Kong, L. (2023). Speech separation algorithm based on comb-filter effect. Applied Acoustics, 203, 109197.

[12] Palani , S. (2023). Finite Digital Filter Design Impulse Response (FIR). In Discrete Time Systems and Signal Processing (pp. 591-732). Cham : Springer International Publishing .

[13] Dhabu , S., Ambede , A., Agrawal , N., Smitha , K.G., Darak , S., & Vinod , A.P. (2020). Variable cutoff frequency FIR filters : A survey. SN Applied Sciences, 2, 1-23.

[14] Wanhammar , L., Saramäki , T., Wanhammar , L., & Saramäki , T. (2020). FIR filter synthesis. Digital Filters Using MATLAB, 163-242.

[15] Harris, F. J. (2022). Multirate signal processing for communications systems. River Publishers.

[16] Owusu , P. (2020). Lowpass filter design microstrip butterworth .

[17] Li, L., Wang, X., Wu , S., & Bian, L. (2021, July). GNSS Receiver Group Delay Measurement Method Based on BOC Signals. In International Conference on Aerospace Systems Science and Engineering (pp. 85-94). Singapore: Springer Nature Singapore.

[18] Palani , S. (2023). IIR Digital Filter Design. In Discrete Time Systems and Signal Processing (pp. 453-590). Cham : Springer International Publishing .

[19] Garg , A., & Sahu, O.P. (2020). A hybrid approach to speech enhancement using wavelet transform Bionic and Butterworth filters . International Journal of Computers and Applications, 42(7), 686-696.

[20] Bellanger , M. (2024). Digital Signal Processing: Theory and Practice . John Wiley & Sons.

[21] Zeng , Y., Nunez , A., & Li, Z. (2022). Speckle noise reduction for structural vibration measurements with vibrometers Laser doppler on a moving platform. Mechanical Systems and Signal Processing, 178, 109196.

[22] Xue , D. (2023). MATLAB and Simulink in Action: Programming, Scientific Computing and Simulation. Spring Nature.

[23] Moler, C., & Little , J. (2020). History of MATLAB. ACM Proceedings on Programming Languages, 4(HOPL), 1-67.

[24] Liu, H., Wang, Z., Zhao , C., Ge , J., Dong , H., & Liu, Z. (2021). Improving the signal to noise ratio of free induction decay signals using a new multilinear single value decomposition based filter . IEEE Transactions on Instrumentation and Measurement, 70, 1-11.

ISSN 2355-3286

Development of Cavendish Banana Maturity Detection and Sorting System Using Open Source Computer Vision and Loadcell Sensor

Achmad Fatchur Rochman[1], Indah Sulistiyowati[2], Jamaaluddin Jamaaluddin[3], Izza Anshory[4]
[1, 2, 3, 4] Teknik Elektro, Universitas Muhammadiyah Sidoarjo, Sidoarjo, Indonesia
[1]rochmanfatchur4137@gmail.com, indah_sulistiyowati@umsida.ac.id, [3]jamaaluddin@umsida.ac.id,
[4]izzaanshory@umsida.ac.id

Accepted 11 November 2024
Approved 12 December 2024

***Abstract*— This research aims to develop a system of detecting the maturity and sorting of cavendish bananas using Open Source Computer Vision (OpenCV) and also assisted by a loadcell sensor. The problem experienced at this time is that fruit sorting is still manual which is less efficient and inaccurate in distinguishing banana maturity based on the color of the skin. This is because the human eye is sensitive to changes in lighting and fatigue. This designed system will use webcam for image processing and loadcell for fruit weight measurement, controlled by Arduino Uno microcontroller. While the algorithm used to determine the color of the ripeness of the banana fruit itself is HSV. The test results show an average weight error of 0.08% for ripe bananas, 0.71& for unripe bananas, while the color detection produces an accuracy of 47.34% on average in bright lighting conditions. In conclusion, this system is successful in improving sorting efficiency with adequate accuracy results, but further development is needed so that the accuracy level increases.**

***Index Terms*— Arduino; Banana Maturity Detector; Loadcell Sensor; OpenCV; Sortation.**

I. Introduction

Banana fruit is a very profitable commodity because it has variety and variety. The nutritional content contained in bananas is very much including sugar, vitamin A, B1, B2, B6, B12 and also vitamin C. Apart from being rich in nutrients, banana fruit can also be processed into various kinds of food, either eaten directly or processed into other products [1], [2].

In addition to having high food value, banana commodities also have high economic value. However, in Indonesia, the treatment of banana trees at the plantation level is less effective. Thus, in terms of banana production in Indonesia has not been able to compete in the international market due to relatively low quality [3].

This is because the detection and sorting tools of this fruit are mostly based on the color of the fruit skin, and the use of sensors used still use TCS3200 which still uses the intensity of light reflected on the object so that the sensor can be read. And the use of this sensor is less effective when the light intensity is less or the object is far from this sensor [4].

The human eye has an amazing ability to detect colors in various lighting conditions. However, adaptation to low light or dark conditions takes time and human vision can be affected by factors such as fatigue. Therefore, the use of OpenCV in performing color detection shows advantages in accuracy and consistency compared to human vision. Studies show that the color conversion from RGB to HSV in image processing is closer to human perception, thus improving the effectiveness of color detection. Under diverse lighting conditions, OpenCV can adapt better, overcoming the limitations faced by the human eye in assessing banana ripeness [5].

Thus, in an effort to increase the level of accuracy and efficiency in sorting bananas, the use of computer vision technology is one of the most promising solutions [6]. Advances in the use of computer vision show great potential for fruit ripeness detection. As in the previous study, which developed a deeo learning-based system with high accuracy that is relevant for other fruits, including bananas [7]. The thing that distinguishes the use of computer vision from previous research with the present is that the previous research used a variety of variables to determine the maturity of the fruit, while the method currently being developed is simpler because it does not require a large data set, so it is more resource efficient. In addition, the research conducted by the author was assisted by using a BLDC motor as a driver of the conveyor so as to improve the performance of the sorting tool [8]. With the help of machine learning algorithms the system can be trained in the form of adding data variations that will improve the performance of the sorting tool [9].

The use of image processing is very diverse not only for the classification of fruit maturity but also for classifying objects around. The use of Python-based OpenCV is also easier for programmers because for classifying the color of cavendish banana ripeness only requires the code of the dominant colors on the banana fruit. Whereas in other studies, classification using different methods still requires a lot of data and the tools made can only do color detection not sorting [10].

In addition to the importance of technology in sorting bananas, it is necessary to provide technical guidance and training to banana farmers who play a key role in the application of modern technology. Research conducted in Gowa and Takalar districts showed that through proper training, farmers can improve their skills in managing post-harvest bananas and adapt to more sophisticated technology, such as the application of technology like OpenCV [11].

OpenCV (Open Source Computer Vision) is one of the libraries on computers as real-time image processing. OpenCV can be applied using the C++, C, Python, and Java programming languages. An example of the application of OpenCV with Python is using a camera mounted on a banana sorting tool that is able to read the ripeness level of the banana fruit. In essence, OpenCV with Python can be utilized for image processing or video processing with the aim that images of bananas can be captured and then processed on a computer. The vision used in OpenCV is not limited to computer cameras, webcam cameras are one option as a substitute for computer cameras that have the same role as vision or as cameras [12], [13].

In addition to the use of the Python library, there are other components that support banana sorting, including the microcontroller used in this sorting tool is Arduino Uno which includes a program for sorting bananas using the C language to move the components in the tool [14], [15].

The driven components include a loadcell sensor this sensor functions in helping sort the banana fruit which if the weight of the ripe banana fruit meets it will be pushed or sorted using a servo motor into the conveyor [16]. Ensuring that the sorted fruit is ripe is assisted by a webcam that uses a Python program that is connected to the Arduino to detect the color level and also open the servo motor to enter the predetermined place [17].

Thus the innovation of this tool is expected to make it easier for farmers when sorting cavendish banana fruit, without checking and classifying the maturity level of cavendish banana fruit. Besides being able to detect the level of maturity, this tool can also sort automatically by using a servo motor as a sorter.

II. Methods

The research method used in this study uses quantitative research methods that focus on the design and realization of the OpenCV Python-based cavendish banana ripeness detection and sorting system. This approach was chosen because of its ability to measure and analyze data objectively, so that it can produce valid and reliable information.

The methods used include observation to identify the problems and needs of the tool, which is essential to ensure that the designed system can meet the expected functional criteria. In addition, conducting literature studies to support understanding in the concept of the tools created, including the use of OpenCV in image processing and color recognition, as has been proven in previous studies [4], [5].

Problem analysis is carried out by systematically testing the tool, which involves collecting data from the loadcell sensor and webcam. This process has the aim of solving problems that may arise during the operation of the tool. Furthermore, data collection and analysis are carried out so that significant conclusions can be drawn regarding the accuracy of the system in detecting fruit ripeness based on predetermined parameters. With this approach, it is expected to increase the efficiency and accuracy of the sorting system, as well as contribute to the development of technology in agriculture and agricultural processing, as in previous studies [1], [6].

A. Block Diagram of System

The main tools used in this research include the use of a webcam as a vision as well as a ripeness detector of banana fruit, assisted by loadcell in classifying the ripeness of the fruit, Arduino Uno as a microcontroller, servo motor for sorting fruit, and other supporting components. The system block diagram can be seen in Fig. 1.

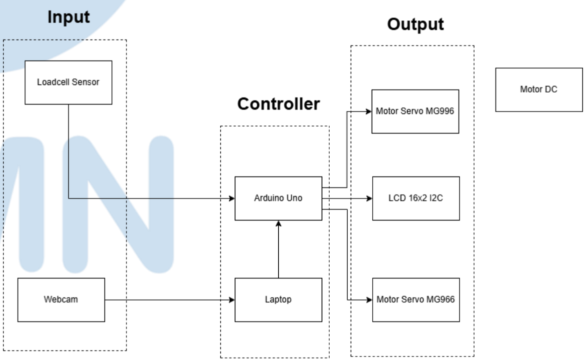

Fig. 1. Block Diagram of System

From Fig. 1 above, the working principle is that the loadcell sensor sends the weight reading data of the ripe or unripe cavendish banana fruit obtained to the Arduino Uno to be processed and displayed on the 16x2 I2C LCD [18]. After that, the first MG966 Servo Motor will move to push the banana into the conveyor and the DC Motor is turned on manually using PWM Motor Speed. The conveyor that turns on carrying bananas when through the vision of the Webcam will be detected the level of ripeness based on the color of the fruit, the data will be sent via a laptop that has a Python program for maturity classification using OpenCV [19]. Data that has been managed with the OpenCV program and algorithm will be sent via Arduino Uno with the output of opening the second MG966 Servo Motor contained in the conveyor [20].

B. Design of Tools and Systems

The prototype of this cavendish banana ripeness detection and sorting tool is made as concisely as possible using two Arduino Uno microcontrollers that have their respective uses as shown in Fig. 2. Is a hardware design design in the form of a sorting conveyor. Fig. 3. Is the result of the tool that has been designed.

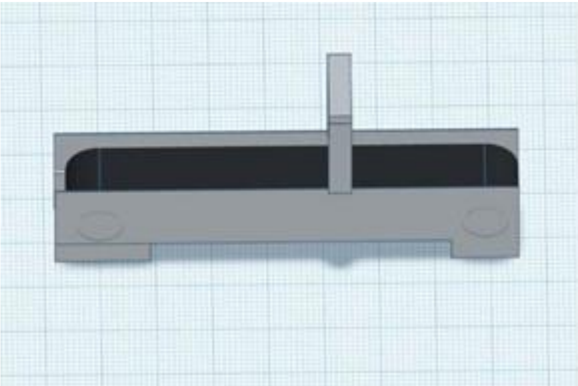

Fig. 2. Design of Sorting Conveyor

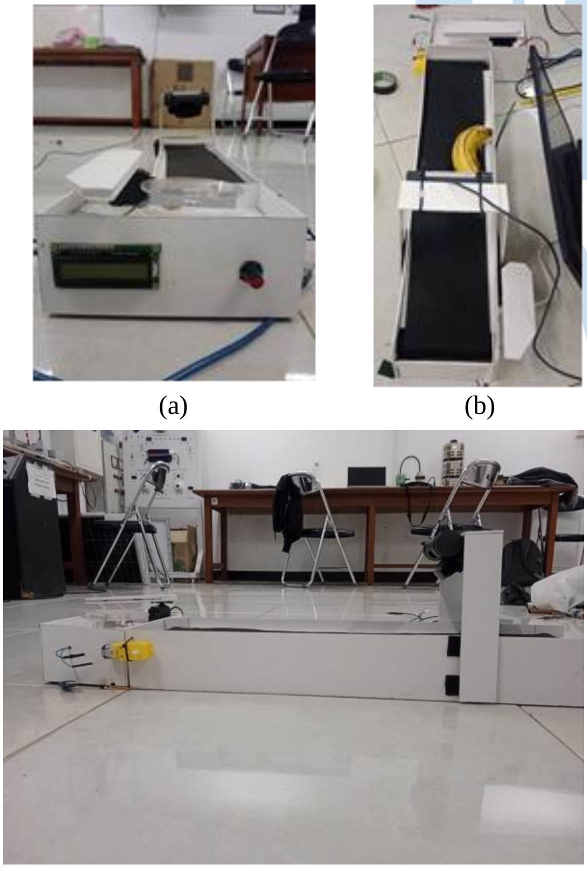

(a) (b)

(c)

Fig. 3. Front View of Tools (a) Top View of Tools (b) and Side View of Tools (c)

In Fig. 2 above shows the design of the hardware while in Fig. 3 is the result of the tool that has been designed where the workings of this tool are as a place to walk the fruit to be sorted using a dc motor as a driver of the conveyor and equipped with a webcam camera that will process the maturity level of the banana fruit but before the fruit enters the conveyor the fruit will be weighed first with a loadcell. The system design of this tool is able to classify the maturity of banana fruit and sorting using machine learning using the OpenCV algorithm. The data used requires a comparison of ripe fruit and unripe fruit by looking at the difference in the color of ripe and unripe fruit. This tool is intended for cavendish banana farmers who have difficulty sorting ripe and unripe bananas. So that in data collection researchers use two comparisons of ripe and unripe fruit.

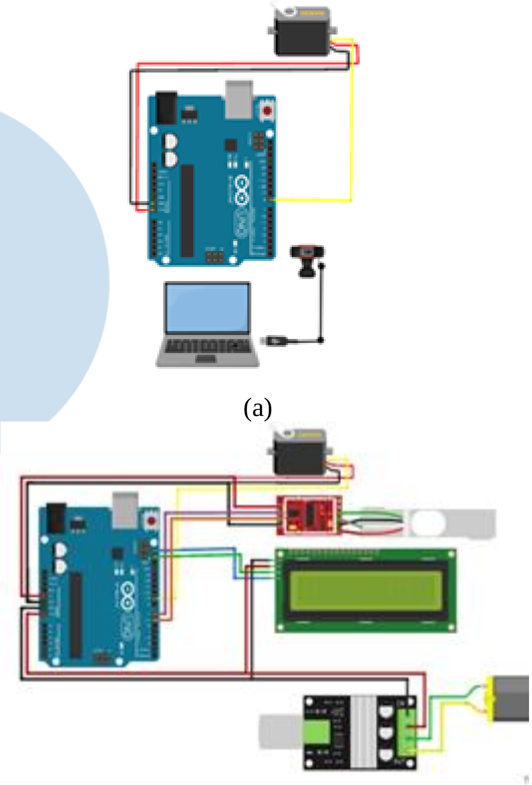

(a)

(b)

Fig. 4. (a) Maturity Detection and Sorting Circuit Schematic Using *OpenCV* (b) Cavendish Banana Fruit Detection Circuit Schematic Using Loadcell

Fig. 4 shows the circuit schematics of each detection device shown in Fig. 4 (a) is a scheme of the circuit that will be filled by the program to detect the level of maturity of the banana fruit that has been obtained the color range. The data is entered into the Python program with the OpenCV library which will be sent to Arduino Uno to activate the servo motor when it detects the ripeness of the banana fruit captured by the webcam camera, and will open the servo on the conveyor for sorting. As for Fig. 4 (b) is a circuit scheme for detecting the level of maturity of banana fruit through changes in weight and texture of banana fruit when the weight has met the criteria for ripe fruit, the servo motor will push the banana fruit that has been weighed using a loadcell sensor into the conveyor.

C. Flowchart

The flowchart depicted in Fig. 5. In the flowchart there are two checking conditions, the first check is the texture or weight of the banana fruit to be sorted because the weight of the unripe banana fruit with the ripe one has a difference, if the predetermined weight is met then the servo contained in the weighing process will actively push the banana fruit into the conveyor, if the weight does not meet then the servo will not move. After the fruit that has entered the conveyor is continued by activating the conveyor by rotating the dc motor pwm, the fruit that is on the conveyor will continue to run until the webcam detects the presence of the fruit and checks the level of maturity with the Python OpenCV program on the computer if the fruit is detected the level of maturity then the servo motor at the end of the conveyor will open for the fruit that passes the sorting.

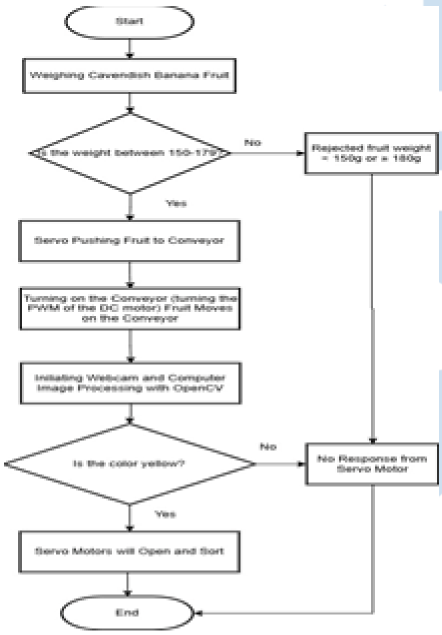

Fig. 5. Flowchart

III. RESULTS AND DISCUSSION

The OpenCV method using HSV color space, which is closer to the perception of the human eye, shows advantages in accuracy as well as flexibility over other methods based on light sensors such as TCS3200, especially in diverse lighting conditions. Compared to using decision trees, the HSV algorithm is simpler and more efficient, although machine learning such as Naïve Bayes can be used to improve the accuracy of more complex datasets.

Data collection was carried out using 30 ripe bananas and 30 unripe bananas. There are 2 kinds of data taken, the first is taking data on the weight of each cavendish banana, and the second is testing the color on the webcam with different light intensities in the room. The tools used to collect this data include digital scales from Idealife and the webcam used from Brio500. From taking these two data, it can be seen as follows:

A. Banana Weight Data Collection

From the data in Table 1 shows the data obtained from measuring the weight of ripe banana fruit, the measurement is carried out once with a total of 30 fruits each so that measurement data is obtained using loadcell scales with kitchen scales. The purpose of this measurement is to know the difference when using kitchen scales and scales made by researchers. Another goal is to know the accuracy of the loadcell scales that have been made by researchers.

TABLE I. WEIGHT MEASUREMENT RESULT OF RIPE BANANA FRUIT

Measurement to	Weight Measurement Result			
	Actual Weight (gram)	Loacell Reading (gram)	Error (gram)	Percent Error (%)
1	157	156.89	0.11	0.07
2	151	150.68	0.32	0.21
3	160	159.92	0.08	0.05
4	161	160.96	0.04	0.02
5	170	169.81	0.19	0.11
6	165	164.95	0.05	0.03
7	162	161.88	0.12	0.07
8	158	157.94	0.06	0.04
9	164	163.98	0.02	0.01
10	171	170.89	0.11	0.06
11	163	162.92	0.08	0.05
12	168	167.87	0.13	0.08
13	160	159.91	0.09	0.06
14	165	164.93	0.07	0.04
15	175	174.61	0.39	0.22
16	170	169.94	0.06	0.04
17	174	173.95	0.05	0.03
18	166	165.92	0.08	0.05
19	159	158.88	0.12	0.08
20	167	166.94	0.06	0.04
21	172	171.89	0.11	0.06
22	169	168.69	0.31	0.18
23	161	160.91	0.09	0.06
24	162	161.89	0.11	0.07
25	164	163.95	0.05	0.03
26	168	167.91	0.09	0.05
27	171	170.88	0.12	0.07
28	160	159.92	0.08	0.05
29	174	174.94	0.94	0.54
30	166	165.91	0.09	0.05
Average			0.14	0.08

The average error obtained is quite small, namely 0.08%, this shows the accuracy of the loadcell scales is not much different from the kitchen scales used during weighing. After testing as many as 30 pieces, the average error reached 0.14. The data in Table 2 measure the weight of banana fruit in raw conditions carried out in the same way using kitchen scales and loadcell scales.

TABLE II. WEIGHT MEASUREMENT RESULT OF RAW BANANA FRUIT

Measurement to	Weight Measurement Result			
	Actual Weight (gram)	Loacell Reading (gram)	Error (gram)	Percent Error (%)
1	205	204.73	0.27	0.13
2	191	189.43	1.57	0.83
3	194	192.16	1.84	0.96
4	184	182.86	1.14	0.62
5	200	200.63	0.63	0.31
6	215	215.66	0.66	0.31
7	200	198.89	1.11	0.55
8	184	185.44	1.44	0.78
9	209	208.45	0.55	0.26
10	230	230.21	0.21	0.09
11	203	202.47	0.53	0.26
12	217	219	2	0.91
13	185	185.32	0.32	0.17
14	180	180.02	0.02	0.01
15	211	212.56	1.56	0.73
16	180	180.77	0.77	0.43
17	184	184.65	0.65	0.35
18	224	223.78	0.22	0.1
19	193	192.28	0.72	0.37
20	208	207.14	0.86	0.42
21	194	193.66	0.34	0.18
22	233	231.78	1.22	0.53
23	190	190.08	0.08	0.04
24	188	187.77	0.23	0.12
25	191	190.64	0.36	0.19
26	201	200.93	0.07	0.05
27	200	199.78	0.22	0.11
28	235	235.68	0.68	0.29
29	197	197.33	0.33	0.17
30	186	185.25	0.75	0.41
Average			0.71	0.36

The error value obtained by unripe fruit is quite large at an average of 0.71%, this is because unripe banana fruit has a denser texture than ripe banana fruit, the measurement results between Table 1 and Table 2 are different because the size of the banana fruit used has a very slight difference. Researchers took measurements again for raw fruit that had turned into ripe fruit and obtained measurement results as in Table 3.

TABLE III. WEIGHT MEASUREMENT RESULT OF RIPE RAW FRUIT

Measurement to	Weight Measurement Result			
	Actual Weight (gram)	Loacell Reading (gram)	Error (gram)	Percent Error (%)
1	201	200.73	0.27	0.13
2	187	186.43	0.57	0.31
3	190	191.16	1.16	0.61
4	181	180.86	0.14	0.08
5	196	195.63	0.37	0.19
6	212	212.66	0.66	0.31
7	196	195.78	0.22	0.11
8	180	181.77	1.77	0.97
9	206	205.44	0.56	0.27
10	226	225.58	0.42	0.19
11	199	198.23	0.77	0.39
12	213	213.01	0.01	0.005
13	181	180.56	0.44	0.24
14	176	175.88	0.12	0.07
15	208	208.37	0.37	0.18
16	178	177.51	0.49	0.28
17	180	180.76	0.76	0.42
18	221	222.54	1.54	0.69
19	189	188.20	0.8	0.43
20	205	204.98	0.02	0.01
21	191	190.08	0.92	0.48
22	229	228.11	0.89	0.391
23	187	187.13	0.13	0.07
24	185	185.41	0.41	0.22
25	187	187.16	0.16	0.09
26	196	196.53	0.53	0.27
27	197	196.61	0.39	0.2
28	230	229.83	0.17	0.07
29	194	194.27	0.27	0.14
30	182	180.78	1.22	0.68
Average			0.47	0.24

In the data in Table 3, no ripe fruit was detected in the tool that the researcher designed this is because the data is new data that has not been entered into the researcher's program. In general, machine learning when new data is inputted, the tool can adapt when experiencing changes as well as what researchers do in this data collection. If you look at the difference from Table 2 and Table 3, the data obtained there is a change in the weight and texture of the banana fruit by 3 - 4 grams. When viewed in Table 1, researchers directly use ripe fruit, it can be assumed that when the fruit is still raw it is also heavier by 3 - 4 grams.

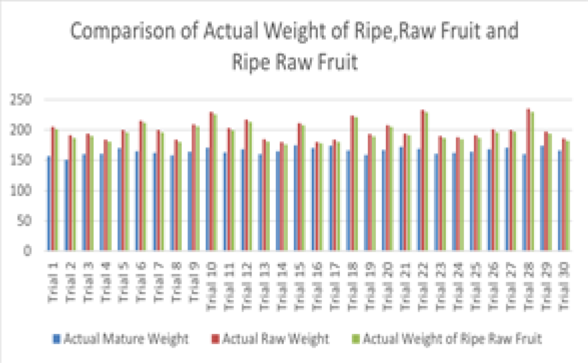

Fig. 6. Comparison of Actual Weight of Ripe, Raw and Ripe Raw Fruit

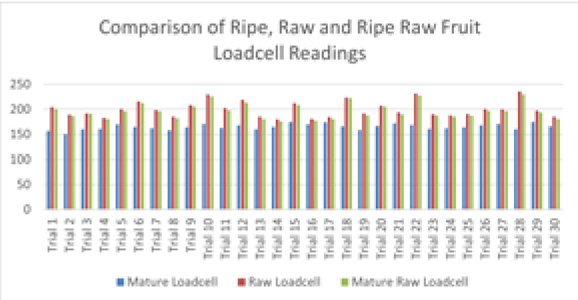

Fig. 7. Comparison of Ripe, Raw and Ripe Raw Fruit Loadcell Readings

When viewed from Fig. 6 and Fig. 7, it shows the difference in actual weight and the difference in loadcell readings from each ripe, unripe and ripe banana fruit. The data in Fig. 6 which is a combination of reading results using digital scales / kitchen scales, while in Fig. 7 is the result of reading from the loadcell scales obtained showing the picture as above.

B. *Data Collection of Banana Fruit Maturity Color*

Data collection for the level of ripeness of banana fruit based on the color of the peel, carried out using a webcam camera connected directly to a computer that has a Python OpenCV program, the detection results will appear on the computer used so that the data can be sent to the Arduino Uno for the sorting process as in Fig. 8. Is the detection of ripe fruit in bright lighting conditions, Fig. 9 is the detection of fruit maturity in dim lighting conditions and Fig. 10 is the detection of fruit maturity in dark conditions.

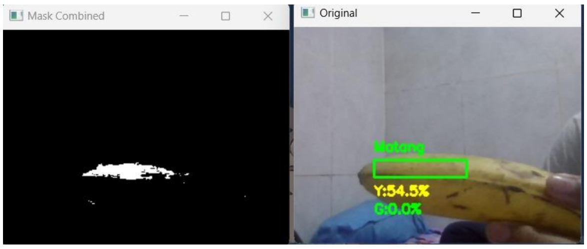

Fig. 8. Data Collection on the Maturity Level of Ripe Banana Fruit in Bright Condition

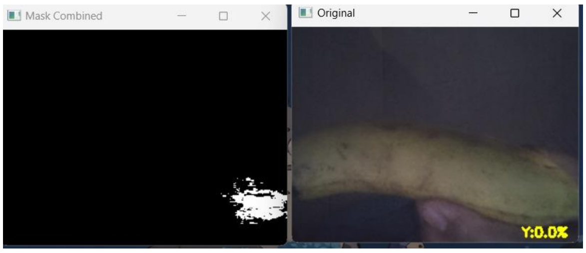

Fig. 9. Data Collection of Ripeness Level of Ripe Banana Fruit in Dim Condition

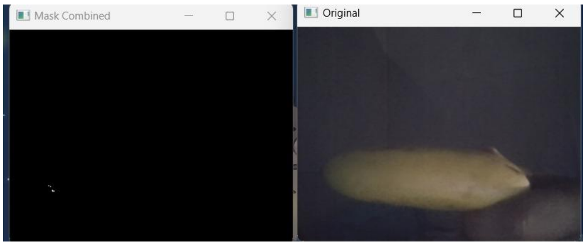

Fig. 10. Data Collection on the Maturity Level of Ripe Banana Fruit in Dark Condition

In the data collection presented in Fig. 8, 9, and 10, it can be seen the difference from the lighting conditions when detecting the color of the banana fruit where the color pixels of the ripe fruit or yellow color are very little detected by the webcam camera. In addition, data collection for the level of ripeness of banana fruit researchers can be seen in Table 4 below how the response of the servo when detected yellow or ripe fruit and the percentage obtained.

TABLE IV. RIPENESS DETECTION TEST RESULT DATA ON RIPE BANANA FRUIT IN BRIGHT LIGHT CONDITION

Measurement to	Accuracy Sensor		
	Servo Response	Detectede Color	Color Percentage
1	Open	Yellow	54.5
2	Open	Yellow	54.5
3	Open	Yellow	49.3
4	Open	Yellow	24.3
5	Open	Yellow	33.6
6	Open	Yellow	50.8
7	Open	Yellow	25.4
8	Open	Yellow	51.4
9	Open	Yellow	62.7
10	Open	Yellow	68.5
11	Open	Yellow	67.5
12	Open	Yellow	50.6
13	Open	Yellow	47.2
14	Open	Yellow	44.8
15	Open	Yellow	40.5
16	Open	Yellow	39.7
17	Open	Yellow	45
18	Open	Yellow	49
19	Open	Yellow	46.3
20	Open	Yellow	44.8

21	Open	Yellow	48.8
22	Open	Yellow	50.8
23	Open	Yellow	50.1
24	Open	Yellow	68.2
25	Open	Yellow	52.4
26	Open	Yellow	55.9
27	Open	Yellow	44.5
28	Open	Yellow	25.7
29	Open	Yellow	22.4
30	Open	Yellow	51.1
Average			47.34

The results of the data obtained when detecting the maturity level of a ripe banana fruit, the average percentage of the color captured is 47.34%. The detected color pixels are affected by other colors besides yellow, therefore when detecting the fruit has a small average value. However, the camera easily captures the color accurately enough for the sorting to run properly.

TABLE V. RIPENESS DETECTION TEST RESULT DATA ON RIPE BANANA FRUIT IN DIM LIGHTING CONDITION

Measurement to	Accuracy Sensor		
	Servo Response	**Detectede Color**	**Color Percentage**
1	Close	Color Not Detected	0
2	Close	Color Not Detected	0
3	Close	Color Not Detected	0
4	Close	Color Not Detected	0
5	Close	Color Not Detected	0
6	Close	Color Not Detected	0
7	Close	Color Not Detected	0
8	Close	Color Not Detected	0
9	Close	Color Not Detected	0
10	Close	Color Not Detected	0
11	Close	Color Not Detected	0
12	Close	Color Not Detected	0
13	Close	Color Not Detected	0
14	Close	Color Not Detected	0
15	Close	Color Not Detected	0
16	Open	Yellow	20.3
17	Open	Yellow	19.1
18	Open	Yellow	22.8
19	Open	Yellow	18.7
20	Open	Yellow	16.4
21	Open	Yellow	15.2
22	Open	Yellow	23.5
23	Open	Yellow	21.8
24	Open	Yellow	19.9
25	Open	Yellow	17.6
26	Open	Yellow	16.2
27	Open	Yellow	20.1
28	Open	Yellow	21
29	Open	Yellow	25
30	Open	Yellow	28.3
Average			10.20

The results obtained when taking data in different lighting conditions get results as in Table 5, where the ripe banana fruit is yellow when in dim lighting conditions the color pixels on the fruit are not detected because the fruit undergoes a color change transition so that the detected yellow color is less. So that the average percentage of color is 10.20% and in this lighting condition the system considers the detected fruit as a ripe fruit because there are few color pixels detected.

TABLE VI. RIPENESS DETECTION TEST RESULT DATA ON RIPE BANANA FRUIT IN DARK LIGHTING CONDITION

Measurement to	Accuracy Sensor		
	Servo Response	**Detectede Color**	**Color Percentage**
1	Close	Color Not Detected	0
2	Close	Color Not Detected	0
3	Close	Color Not Detected	0
4	Close	Color Not Detected	0
5	Close	Color Not Detected	0
6	Close	Color Not Detected	0
7	Close	Color Not Detected	0
8	Close	Color Not Detected	0
9	Close	Color Not Detected	0
10	Close	Color Not Detected	0
11	Close	Color Not Detected	0
12	Close	Color Not Detected	0
13	Close	Color Not Detected	0
14	Close	Color Not Detected	0
15	Close	Color Not Detected	0

16	Close	Color Not Detected	0
17	Close	Color Not Detected	0
18	Close	Color Not Detected	0
19	Close	Color Not Detected	0
20	Close	Color Not Detected	0
21	Close	Color Not Detected	0
22	Close	Color Not Detected	0
23	Close	Color Not Detected	0
24	Close	Color Not Detected	0
25	Close	Color Not Detected	0
26	Close	Color Not Detected	0
27	Close	Color Not Detected	0
28	Close	Color Not Detected	0
29	Close	Color Not Detected	0
30	Close	Color Not Detected	0
Average			0

The data results in Table 6 are not much different from the results in Table 5. The difference between these two data is the lighting conditions of the data collection on the fruit. It shows that the yellow color pixel of the fruit is not detected on the camera so that the average percentage of the color is 0% which makes the servo not open. In this condition color detection is almost impossible for the camera to identify the color.

The data taken for banana fruit in unripe condition with the same lighting conditions as in Fig. 11 for ripeness detection on unripe fruit in bright conditions, Fig. 12 for ripeness detection in dim lighting conditions, and Fig. 13 for ripeness detection in dark light conditions.

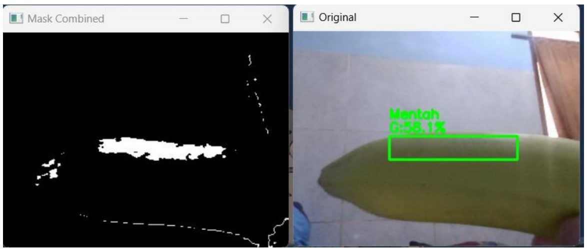

Fig. 11. Data Collection of Maturity Level of Raw Banana Fruit in Bright Condition

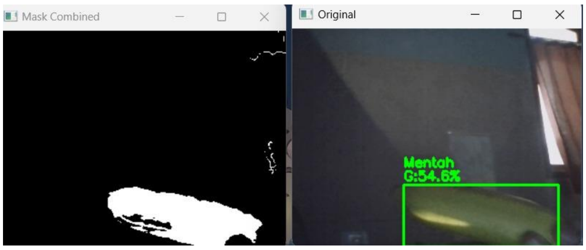

Fig. 12. Data Collection of Maturity Level of Banana Fruit in Dim Condition

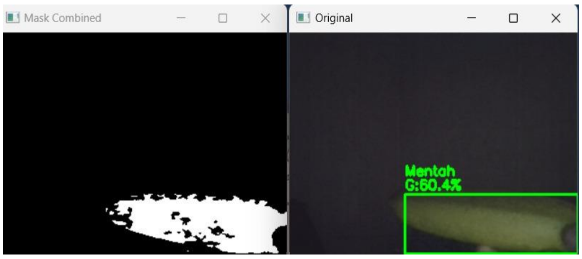

Fig. 13. Data Collection on the Maturity Level of Raw Banana Fruit in Dark Condition

At the time of data collection, bright light conditions were detected to be ripe because there was a yellow color and also the banana fruit itself was greenish yellow but the weight of this banana fruit did not meet the requirements and did not want to enter the conveyor as shown in Fig. 11, 12 and 13 of the fruit detected by the webcam. However, from the data collection, the servo motor also experienced a response when the fruit was detected to be greenish yellow as shown in Table 7.

TABLE VII. Ripeness Detection Test Result Data on Raw Banana Fruit in Bright Lighting Condition

Measurement to	**Accuracy Sensor**		
	Servo Response	**Detectede Color**	**Color Percentage**
1	Close	Green	54.4
2	Close	Green	58.1
3	Close	Green	58.5
4	Close	Green	56.4
5	Close	Green	55.9
6	Close	Green	54.7
7	Close	Green	57.3
8	Close	Green	51.1
9	Close	Green	55.4
10	Close	Green	58.8
11	Close	Green	57.3
12	Close	Green	59.1
13	Close	Green	56.2
14	Close	Green	58.7
15	Close	Green	60
16	Close	Green	55.5
17	Close	Green	57.8
18	Close	Green	54.9
19	Close	Green	59.3

20	Close	Green	58.4
21	Close	Green	56.7
22	Close	Green	58.2
23	Close	Green	55.6
24	Close	Green	54.7
25	Close	Green	57.9
26	Close	Green	57.2
27	Close	Green	60.4
28	Close	Green	43.3
29	Close	Green	54.8
30	Close	Green	56.7
Average			56.44

The results obtained in Table 7 after testing the color detection of banana fruit in bright lighting conditions the detected color is green with an average color detected depending on the color pixel is 56.44% and detected that the fruit is still unripe. As shown in Fig. 11, the detected fruit is dominantly green which causes the percentage of detected colors to be quite large.

TABLE VIII. RIPENESS DETECTION TEST RESULT DATA ON RAW BANANA FRUIT IN DIM LIGHTING CONDITION

Measurement to	**Accuracy Sensor**		
	Servo Response	**Detectede Color**	**Color Percentage**
1	Close	Green	59.8
2	Close	Green	52.2
3	Close	Green	51.4
4	Close	Green	55.5
5	Close	Green	54.6
6	Close	Green	51.1
7	Close	Green	45.8
8	Close	Green	30.9
9	Close	Greenish Yellow	59.7
10	Close	Green	60.4
11	Close	Green	36.6
12	Close	Green	58.2
13	Close	Green	47.3
14	Close	Green	59.2
15	Close	Green	52.2
16	Close	Green	51.4
17	Close	Green	55.5
18	Close	Green	54.6
19	Close	Green	53.7
20	Close	Green	56.3
21	Close	Green	57.8
22	Close	Green	52.1
23	Close	Green	55.9
24	Close	Green	56.5
25	Close	Green	54.0
26	Close	Green	53.2
27	Close	Green	57.4
28	Close	Green	54.4
29	Close	Green	52.2
30	Close	Green	51.4
Average			52.94

In Table 8 data, it has been tested to detect the maturity of banana fruit in low light conditions, it is found that the webcam camera detects the green color on the banana fruit, the green color pixels detected in the fruit test get an average value of 52.94%, this is because the dominant color detected is still visible as in dim lighting. As in Fig. 12 each fruit has a fairly high percentage because the color pixels that are read are quite a lot.

TABLE IX. RIPENESS DETECTION TEST RESULT DATA ON RAW BANANA FRUIT IN DARK LIGHTING CONDITION

Measurement to	**Accuracy Sensor**		
	Servo Response	**Detectede Color**	**Color Percentage**
1	Close	Green	57.2
2	Close	Greenish Yellow	54.4
3	Close	Green	55.9
4	Close	Green	60.4
5	Close	Color Not Detected	0
6	Close	Green	36.2
7	Close	Green	58.4
8	Close	Green	30.2
9	Close	Green	28.1
10	Close	Green	25.5
11	Close	Green	29.8
12	Close	Green	45.2
13	Close	Green	35.8
14	Close	Green	47.1
15	Close	Green	44.5
16	Close	Green	21.9
17	Close	Green	57.2
18	Close	Green	55.9
19	Close	Green	50.3
20	Close	Green	40.6
21	Close	Color Not Detected	0
22	Close	Green	27.3
23	Close	Green	31.1
24	Close	Green	59.1
25	Close	Green	30.3
26	Close	Color Not Detected	0
27	Close	Green	46.8
28	Close	Green	48.4
29	Close	Green	58.4
30	Close	Color Not Detected	0

Average	37.87

The data in Table 9 is almost the same as the previous raw fruit data, the difference is that when taking data in dark light conditions there are yellow-green color readings and some are not detected by the camera from the webcam. Pixel color from yellow is 24.4% and green is 30% so that the average color is obtained by 37.87% when totaled as a whole percentage of the data taken. The average of the fruit detected in this dark condition is the green color pixel which is more dominant than the yellow color pixel on the fruit. The difference can be seen in Fig. 13 above is a portion of the color captured with a relatively small percentage of color due to lighting that affects the ability of the webcam camera to detect color.

After taking data for the accuracy of the sensor with the response of the servo motor can be displayed in the form of a graph for the average value obtained from testing in bright, dim, and dark lighting conditions for ripe fruit and unripe fruit with the same lighting conditions can be seen through the graph presented below:

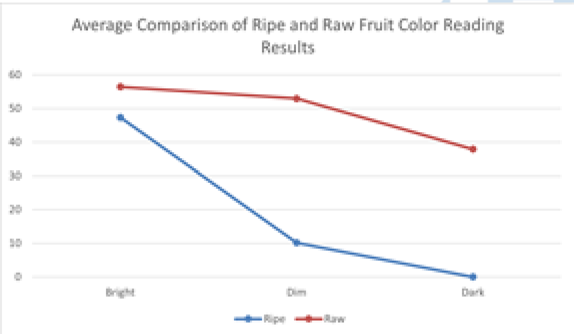

Fig. 14. Graph of Average Sensor Readings

The difference obtained through this detection shows that light conditions play a significant role in the accuracy of the system. To further understand the advantages and disadvantages of the various methods that can be used in fruit ripeness detection systems, please refer to the table presented below:

TABLE X. COMPARISON OF THE ADVANTAGES AND DISADVANTAGES OF THE MENTIONED METHODS

Methods	Advantage	Shortage
TCS3200	Simple	Less effective in low light conditions
Decision Tree	Fast for small datasets	Unsuitable for complex datasets
OpenCV	Accurate and flexible	Performance degrades in dark lighting
Naive Bayes	Adaptive for diverse data	Requires large datasets

A conclusion can be drawn for the use of the methods mentioned, that using the OpenCV method was chosen by the author due to its advantages in flexibility and accuracy in color detection, which is relevant to the needs of the developed tool. However, combining it with other methods such as Decision Tree or Naïve Bayes can improve the performance of the tool if the dataset is larger or with additions such as reading the texture of the fruit.

C. *Limitation and Future Work*

The system developed in this study has several limitations that need to be considered. One of the main limitations of this research is the sensitivity to lighting conditions, the accuracy of color detection decreases due to low or dark lighting, as shown in table 4, the results are 47.34% in bright conditions, but in dim conditions 10.2% and 0% in dark conditions. To improve performance in the future, it can be done by adding datasets with more variations and implementing adaptive algorithms on HSV parameters to increase accuracy in various lighting conditions.

D. *Comparison with Similar Systems*

The system proposed by the authors uses OpenCV to perform banana ripeness detection based on skin color, which is more flexible and efficient than using TCS3200 and Decision Tree. OpenCV offers higher accuracy in various lighting conditions by utilizing HSV color space, while the use of TCS3200 sensor is more sensitive to light changes. While Decision Tree is fast on small datasets, it is less adaptive to complex data variations. Another study using a different method, Naïve Bayes, showed superiority on large datasets, but required more resources. The results of this test show an accuracy of 47.34% in bright conidia which can still be improved with algorithm adjustments. This system provides a simple and efficient solution compared to more complex machine learning-based methods, with potential for further development.

IV. CONCLUSION

This banana ripeness detection and sorting tool has been successfully realized, the tool succeeds in recognizing changes in texture and weight of ripe and unripe cavendish bananas. OpenCV which works as a maturity level detector can also classify the maturity of banana fruit based on the color of the fruit. From the test results that have been carried out this tool has an average error for reading the weight of the fruit of 0.09%, 0.57%, and 0.26% respectively.

The test results of this tool that have been realized show that the level of accuracy is fairly sufficient, but this tool needs to be developed by adding training data so that this tool can function better in the hope of increasing the accuracy of this tool in classifying either from color or from the weight or texture of the fruit.

REFERENCES

[1] B. S. Purwokol and K. Suryana, "Efek Suhu Simpan dan Pelapis terhadap Perubahan Kualitas Buah Pisang

Cavendish," *Bul. Agron*, vol. 28, no. 3, pp. 77–84, 2020.
[2] R. Arifuddin, S. Subairi, A. B. Setiawan, M. A. Ridlo, and A. N. Ziliwu, "Determining PID Parameters For Temperature Control System in Cavendish Banana Storage Room," *JEEE-U (Journal Electr. Electron. Eng.*, vol. 8, no. 1, pp. 15–23, 2024, doi: 10.21070/jeeeu.v8i1.1683.
[3] A. L. Baihaqi, T. P. Fiqar, and B. M. Pratama, "Klasifikasi Kematangan Musa Paradisiaca L Berbasis Warna Kulit Menggunakan Metode Decision Tree," *J. Borneo Inform. dan Tek. Komput.*, vol. 3, no. 2, pp. 14–22, 2023, doi: 10.35334/jbit.v3i2.3317.
[4] M. F. Ajizi, D. Syauqy, M. Hannats, and H. Ichsan, "Klasifikasi Kematangan Buah Pisang Berbasis Sensor Warna Dan Sensor Load Cell Menggunakan Metode Naive Bayes," *J. Pengemb. Teknol. Inf. dan Ilmu Komput.*, vol. 3, no. 3, pp. 2472–2479, 2019, [Online]. Available: https://j-ptiik.ub.ac.id/index.php/j-ptiik/article/view/4692
[5] M. Z. Andrekha and Y. Huda, "Deteksi Warna Manggis Menggunakan Pengolahan Citra dengan Opencv Python P - ISSN : 2302-3295," vol. 9, no. 4, 2021.
[6] H. Muchtar and R. Apriadi, "Implementasi Pengenalan Wajah Pada Sistem Penguncian Rumah Dengan Metode Template Matching Menggunakan Open Source Computer Vision Library (Opencv)," *Resist. (elektRonika kEndali Telekomun. tenaga List. kOmputeR)*, vol. 2, no. 1, p. 39, 2019, doi: 10.24853/resistor.2.1.39-42.
[7] M. Faisal, F. Albogamy, H. Elgibreen, M. Algabri, and F. A. Alqershi, "Deep Learning and Computer Vision for Estimating Date Fruits Type, Maturity Level, and Weight," *IEEE Access*, vol. 8, no. Fig. 1, pp. 206770–206782, 2020, doi: 10.1109/ACCESS.2020.3037948.
[8] I. Anshory, I. Robandi, and M. Ohki, "System Identification of BLDC Motor and Optimization Speed Control Using Artificial Intelligent," *Int. J. Civ. Eng. Technol.*, vol. 10, no. 7, pp. 1–13, 2019, [Online]. Available: http://www.iaeme.com/ijciet/issues.asp?JType=IJCIET&VType=10&IType=7http://www.iaeme.com/IJCIET/issues.asp?JType=IJCIET&VType=10&IType=7
[9] A. Roihan, P. A. Sunarya, and A. S. Rafika, "Pemanfaatan Machine Learning dalam Berbagai Bidang: Review paper," *IJCIT (Indonesian J. Comput. Inf. Technol.*, vol. 5, no. 1, pp. 75–82, 2020, doi: 10.31294/ijcit.v5i1.7951.
[10] Y. Amrozi, D. Yuliati, A. Susilo, N. Novianto, and R. Ramadhan, "Klasifikasi Jenis Buah Pisang Berdasarkan Citra Warna dengan Metode SVM," *J. Sisfokom (Sistem Inf. dan Komputer)*, vol. 11, no. 3, pp. 394–399, 2022, doi: 10.32736/sisfokom.v11i3.1502.
[11] Waryat and Nurjanani, "Efektivitas Bimbingan Teknis Budidaya Dan Pengolahan Pisang Terhadap Peningkatan Pengetahuan Dan Respon Petani Di Kabupaten Gowa Dan Takalar, Sulawesi Selatan," *Pros. Semin. Nas. Has. Penelit. Agribisnis VI*, no. 1, pp. 447–452, 2022, [Online]. Available: https://jurnal.unigal.ac.id/index.php/prosiding/article/view/7766%0Ahttps://jurnal.unigal.ac.id/index.php/prosiding/article/download/7766/4909
[12] R. Isum, S. Maryati, and B. Tryatmojo, "Raden Isum Suryani Maryati Akurasi Sistem Face Recognition Akurasi Sistem Face Recognition OpenCV Menggunakan Raspberry Pi Dengan Metode Haar Cascade KATA KUNCI Akurasi Face Recognition Raspberry Pi OpenCV Haar Cascade," *J. Ilm. Inform.*, no. Cv, p. 12790, 2019.
[13] I. Sulistiyowati and M. I. Muhyiddin, "Disinfectant Spraying Robot to Prevent the Transmission of the Covid-19 Virus Based on the Internet of Things (IoT)," *J. Electr. Technol. UMY*, vol. 5, no. 2, pp. 61–67, 2021, doi: 10.18196/jet.v5i2.12363.
[14] Jamaaluddin, A. Akbar, and Khoiri, "Ultrasonic Flow Meters and Microcontrollers for Precise Water Management with 6.45% Error Margin," *IOP Conf. Ser. Earth Environ. Sci.*, vol. 1242, no. 1, 2023, doi: 10.1088/1755-1315/1242/1/012017.
[15] A. Ahfas, M. B. Ulum, D. H. R. Saputra, and S. Syahrorini, "Automatic Spray Desinfectant Chicken with Android Based on Arduino Uno," *IOP Conf. Ser. Earth Environ. Sci.*, vol. 519, no. 1, 2020, doi: 10.1088/1755-1315/519/1/012013.
[16] M. F. Laksono Hadi, I. Sulistiyowati, J. Jamaaluddin, and I. Anshory, "Design of a Height and Weight Measurement Tool for Toddlers at Spreadsheet-Based Posyandu," *JEEE-U (Journal Electr. Electron. Eng.*, vol. 7, no. 2, pp. 163–175, 2023, doi: 10.21070/jeeeu.v7i2.1677.
[17] A. Basrah Pulungan, Z. Nafis, M. Anwar, D. Elvanny Myori, and N. Padang, "Object Detection With a Webcam Using the Python Programming Language," *J. Appl. Eng. Technol. Sci.*, vol. 2, no. 2, pp. 103–111, 2023.
[18] I. Sulistiyowati, H. M. Ichsan, and I. Anshory, "Konveyor Penyortir Objek Dengan Deteksi Warna Menggunakan Kamera Esp-32," vol. 4, no. 1, 2024.
[19] F. E. Saputra, R. Cahya Wihandika, and A. W. Widodo, "Penentuan Kualitas Biji Kopi Menggunakan Local Ternary Patterns Dan RGB-HSV Color Moment Dengan Learning Vector Quantization," *J. Pengemb. Teknol. Inf. dan Ilmu Komput.*, vol. 5, no. 6, pp. 2299–2307, 2021, [Online]. Available: http://j-ptiik.ub.ac.id
[20] D. S. Febriyan and R. D. Puriyanto, "Implementation of DC Motor PID Control on Conveyor for Separating Potato Seeds by Weight," *Int. J. Robot. Control Syst.*, vol. 1, no. 1, pp. 15–26, 2021, doi: 10.31763/ijrcs.v1i1.221.
.

ISSN 2355-3286

Air Filtration System Utilizing Biomimetic Technology and IoT for Air Quality Improvement

Mochamad Rizal Fauzan[1], Silmi Ath Thahirah Al Azhima[2], Resa Pramudita[3], Dadang Lukman Hakim[4], Hanifah Indah Rahmawati[5], Mutiara Nabila Azmi[6], Rafi Rahman Fauzi[7], Maman Somantri[8], Sri Rahayu[9]
[1,7,8] Pendidikan Teknik Elektro, UPI, Bandung, Indonesia
[2,3] Pendidikan Teknik Otomasi Industri dan Robotika, UPI, Bandung, Indonesia
[4] Teknik Elektro, UPI, Bandung, Indonesia
[5,6,9] Pendidikan Teknik Bangunan, UPI, Bandung, Indonesia
[1]rizalfauzan@upi.edu, [2]silmithahirah@upi.edu, [3]resa.pd@upi.edu, [4]dadanglh@upi.edu, [5]hanifahindah08@upi.edu, [6]mutiaranabila08@upi.edu, [7]rafi.zahranf@upi.edu, [8]msomantri@upi.edu, [9]srirahayu@upi.edu

Accepted 11 November 2024
Approved 09 December 2024

***Abstract*— The "Hepix" smart air filtration system, developed with biomimetic and Internet of Things (IoT) technology, aims to address the urgent issue of poor indoor air quality, particularly in high-mobility urban areas. This system integrates advanced sensors (MQ135 and BME680) and biomimetic filtration inspired by leaf stomata to monitor and filter air pollutants. Tested across three locations—Cilame, Jatinangor, and Cibiru—the system achieved an approximate 24.4% reduction in pollutant levels, as well as stable control of humidity and air pressure. Real-time data is continuously monitored through a mobile and web interface, supported by Google Assistant integration for voice commands. The results demonstrate that "Hepix" effectively improves air quality, offering a practical solution for healthier indoor environments in urban areas.**

***Index Terms*— Air filtration; biomimetic technology; Internet of Things; indoor air quality.**

I. Introduction

Urban air quality has become an increasingly urgent environmental issue. The rising emissions from motor vehicles, industries, and other human activities have led to a significant decline in air quality. According to an IQAir report in July 2024, Indonesia ranks third out of 116 countries with the highest levels of air pollution in the world, with most of this pollution concentrated in urban areas with dense industrial activities [1][2]. The impact of this air pollution is not limited to the environment but also has serious health consequences, including an increased risk of chronic respiratory diseases such as asthma, bronchitis, and even lung cancer [3][4].

Amid this urgency, the development of technologies to improve indoor air quality has become crucial. Several innovations have been developed to filter and enhance air quality, such as the "Smart Air Purifier" system [5], which uses an MQ135 sensor and Arduino Uno to monitor and filter air particles. However, this study revealed some limitations, such as the device's inability to identify the type of pollutants being filtered and a design that is less portable and practical for everyday use [6].

Another study about developed an indoor air quality monitoring system using a microcontroller and an Android application [7][8]. Although this device provides a good monitoring solution, limitations such as the Bluetooth signal range of only about 10 meters and the lack of integration with AC power make this system less optimal for wider urban use [9][10]. This indicates a need for more advanced and comprehensive solutions to address indoor air quality challenges [11].

To address these limitations, this research offers the development of a smart air filtration system based on biomimetic and Internet of Things (IoT) technology, named "Hepix." This system not only filters the air but also monitors air quality in real time through the integration of advanced sensors such as the MQ135 and BME680 [12][13]. The biomimetic technology employed mimics the natural mechanism of leaf stomata, which effectively manages gas exchange in plants, to be applied in air filtration. IoT integration allows continuous air quality monitoring and control through a smartphone-based application, enabling users to access air quality information and operate the system remotely [14][15].

Furthermore, the system is integrated with Google Assistant, allowing users to activate or deactivate the system through voice commands. This feature provides added convenience and ease of use in daily life, especially for those living in areas with varying air quality [16]. This study aims to develop and test the effectiveness of a smart air filtration system based on biomimetic and IoT technology in improving indoor air quality in urban environments. Through this approach, it is expected to provide a more effective and efficient solution to indoor air pollution problems, while also contributing new insights into the application of biomimetic and IoT technology for environmental health [17].

II. METHOD

This section describes the development process of the "Hepix" air filtration system, covering system architecture, hardware design, and software design. Each element is designed to ensure the system can effectively monitor and improve indoor air quality [18].

A. System Architecture and Flowchart

The system architecture of "Hepix" illustrates the structure and interaction between key components, such as advanced sensors and IoT integration, enabling real-time air quality monitoring and filtration. The architecture diagram Fig 1 shows the main elements, including the MQ135 and BME680 sensors, microcontroller, and IoT framework, which allow for remote monitoring and control.

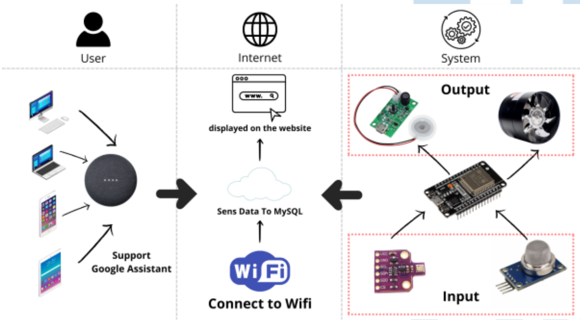

Fig. 1. Architecture system design

The flowchart Fig 2 outlines the operational flow from initial air quality detection, through filtration, to real-time data updates on the user interface. This diagram demonstrates the logical sequence of data collection, processing, and user notifications, showing how each component works together to improve air quality.

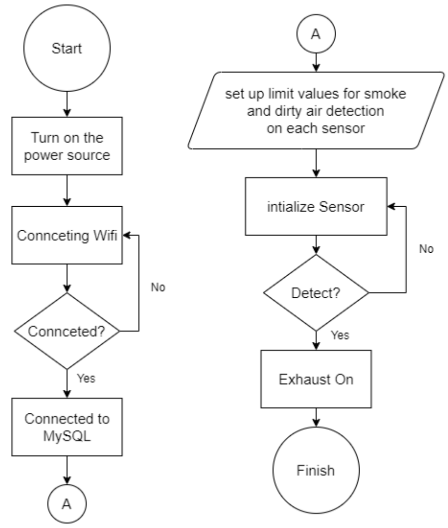

Fig. 2. Flowchart system

B. Hardware Design

The hardware design of the "Hepix" system includes the detailed specifications of the physical components necessary for effective air filtration and air quality monitoring. This includes sensors like MQ135 and BME680, essential for measuring pollutants and environmental parameters. Fig 3 provides the schematic design, illustrating the circuit connections and how each component is integrated to function cohesively within the system.

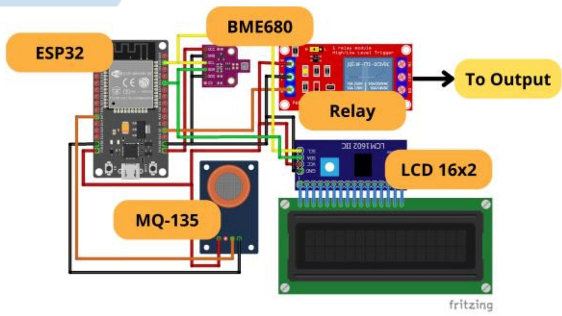

Fig. 3. Schematic Design

Additionally, Fig 4 shows the 3D product design, highlighting the physical layout and structural arrangement to ensure the device is both portable and user-friendlyand in Fig 5 is the realization of the tool. This design approach aims to enhance the practical usability of the system in various indoor environments, facilitating easier deployment and maintenance, and product.

ISSN 2355-3286

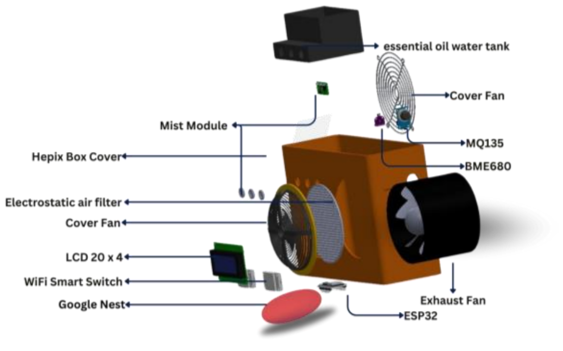

Fig. 4. Design 3D Product

Fig. 5. Realization Product

C. *Software Design*

The software design incorporates programming for data acquisition, processing, and communication with the user interface. Fig 6 presents the software system architecture as implemented on the web interface, displaying the data flow from sensors to the MySQL database and further to the user application. This design enables seamless interaction between the device and the IoT framework, allowing for continuous air quality monitoring and control through the web interface.

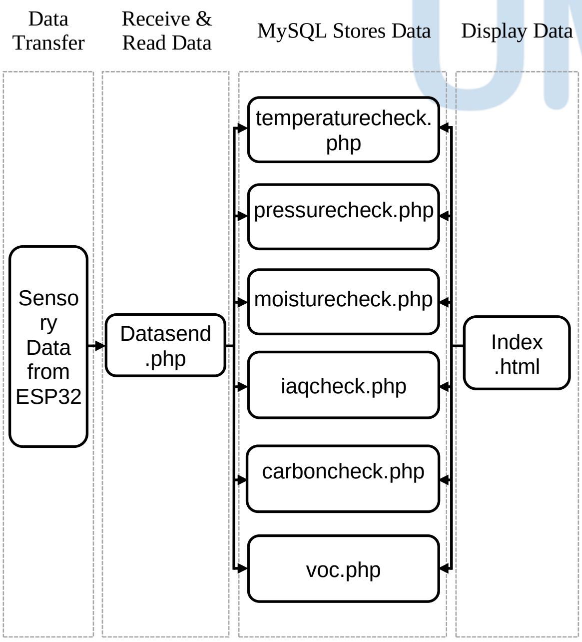

Fig. 6. Architecture software system design on website

Further details on data management are shown in Fig 6, which illustrates the MySQL database structure. This database stores real-time air quality data, which can be accessed and displayed through the user application. The integration of Google Assistant also provides voice-command functionality, offering users a convenient and hands-free way to interact with the system.

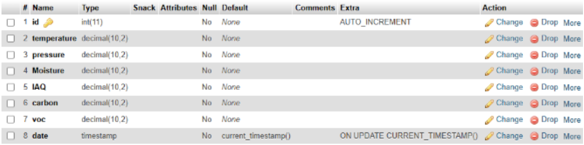

#	Name	Type	Snack	Attributes	Null	Default	Comments	Extra	Action
1	id	int(11)			No	None		AUTO_INCREMENT	Change Drop More
2	temperature	decimal(10,2)			No	None			Change Drop More
3	pressure	decimal(10,2)			No	None			Change Drop More
4	Moisture	decimal(10,2)			No	None			Change Drop More
5	IAQ	decimal(10,2)			No	None			Change Drop More
6	carbon	decimal(10,2)			No	None			Change Drop More
7	voc	decimal(10,2)			No	None			Change Drop More
8	date	timestamp			No	current_timestamp()		ON UPDATE CURRENT_TIMESTAMP()	Change Drop More

Fig. 7. MySQL Data

III. Testing And Result

This section presents the testing process and results of the "Hepix" air filtration system, conducted in three different regions: Cilame, Jatinangor, and Cibiru. Each location was selected to represent distinct environmental conditions, providing a comprehensive evaluation of the system's effectiveness in diverse indoor settings. The tests focused on key metrics, including functional testing, humidity, air quality index, air pressure, and a comparative analysis of pollutant concentration (PPM) before and after using the device.

The tests were conducted in a living room with a size of 15 m² (or 45 m³), which was selected as the optimal room size for the air filtration system. This room size represents a typical indoor environment in residential areas, providing a controlled setting that mirrors common living conditions. The living room was chosen specifically because it is closest to the external environment, allowing for a more accurate comparison between indoor air quality and outdoor conditions. During the tests, the room was maintained under typical residential conditioning scenarios, with the air conditioning and ventilation systems operating at standard settings, ensuring that the results reflect realistic usage conditions.

A. *Functional Testing Results*

The initial functional testing was conducted to ensure that each component of the "Hepix" system operated as intended. This included testing sensor accuracy, device responsiveness, and IoT connectivity. Table I summarizes the functionality test results, detailing the performance and reliability of each system component under various conditions.

TABLE I. Functionality Testing

Component	Functionality	Result	Remarks
MQ135 Sensor	Detect air pollutants (CO_2, NH_3)	Pass	Responsive to pollutant levels

BME680 Sensor	Measure temperature and humidity	Pass	Stable measurements
Microcontroller	Data processing and sensor control	Pass	No delay in data processing
IoT Module	Connects to mobile app and website	Pass	Consistent connection with app and website
Biomimetic-Based Air Filtration	Filter out indoor pollutants	Pass	Effective reduction in PPM levels
Google Assistant	Voice activation	Pass	Commands executed accurately
Power Supply	Continuous power delivery	Pass	Suitable for long-term operation

B. *Humidity*

The humidity measurements in Jatinangor, Cibiru, and Cilame show varying average levels, with Jatinangor at 80.1%, Cibiru at 77.3%, and Cilame at 73.1%. The graph illustrates daily humidity fluctuations across these locations, highlighting the "Hepix" system's ability to adapt to different environmental conditions in maintaining balanced indoor humidity show in Fig 8.

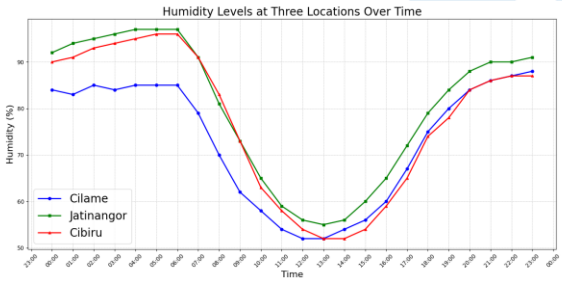

Fig. 8. Humidty Graph

C. *Air Quality Index (AQI)*

The AQI measurements across Jatinangor, Cibiru, and Cilame show average values of 67.5%, 68.4%, and 68.7%, respectively. The graph illustrates variations in AQI levels throughout the day, reflecting fluctuations in air quality across these locations. This data helps assess the "Hepix" system's capability to respond to changes in air quality and improve indoor environments effectively, as shown in Fig 9.

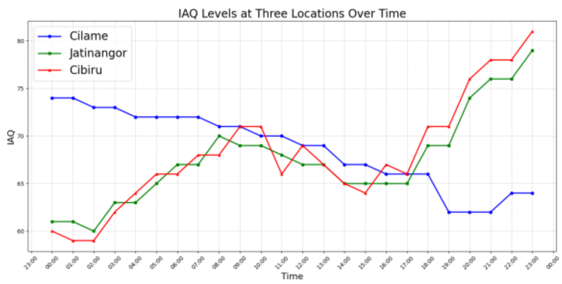

Fig. 9. AQI Graph

D. *Air Pressure*

Air pressure measurements across Jatinangor, Cibiru, and Cilame show average values of 1003.07 hPa, 1013.98 hPa, and 929.28 hPa, respectively. The graph illustrates the stability of air pressure over time at each location, indicating minor fluctuations throughout the day. This data, as shown in Fig 10, helps evaluate the "Hepix" system's ability to operate effectively under varying environmental pressures.

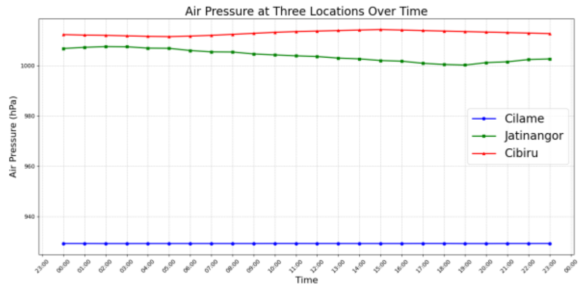

Fig. 10. Air Pressure Graph

E. *Comparative PPM Graph: Before and After Using the Device*

A comparative analysis of pollutant concentration (PPM) levels on July 2 and July 3 highlights the system's effectiveness in reducing indoor air pollution. The highest PPM recorded on July 2 was 742, which decreased to 561 on July 3, a reduction of approximately 24.4%. This reduction illustrates the "Hepix" system's capability to significantly lower pollutant levels, providing a healthier indoor environment by filtering airborne contaminants over time, as shown in Fig 11.

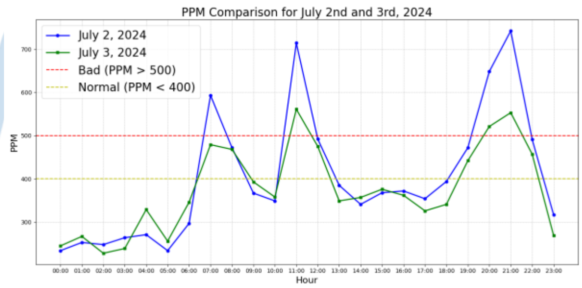

Fig. 11. Comparative PPM Graph

F. *Software Result*

Fig. 12. Hepix system dashboard

The "Hepix" system's software dashboard, as shown in Fig 12, provides real-time monitoring of key environmental parameters, including temperature, pressure, humidity, and pollutant concentrations (e.g., CO_2, CO, and VOCs) in PPM. This web-based interface enables users to track indoor air quality metrics efficiently, allowing for timely responses to changing conditions. The intuitive design and clear display ensure that users can easily interpret data and make informed decisions about their indoor environment.

IV. Conclusion

The development and testing of the "Hepix" smart air filtration system, which integrates biomimetic and IoT technology, highlight its effectiveness in enhancing indoor air quality across varied environmental conditions. Conducted in three locations with high mobility and diverse air quality challenges Cilame, Jatinangor, and Cibiru the study demonstrated the system's adaptability and robustness in maintaining healthy indoor environments. The "Hepix" system achieved a notable pollutant concentration reduction of approximately 24.4%, showcasing its ability to significantly improve air quality. Functional tests confirmed the reliability of all components, including pollutant and environmental sensors, IoT connectivity for real-time monitoring, and Google Assistant integration for hands-free operation. These results position the "Hepix" system as a promising solution to address urban indoor air pollution, offering practical applications that support healthier, safer living spaces through continuous air quality monitoring and filtration.

Acknowledgment

The authors would like to express their gratitude to the Ministry of Education and Culture's Directorate General of Higher Education (SIMBELMAWA) for funding this research through the 2024 Student Creativity Program (Program Kreativitas Mahasiswa) under the Karsa Cipta (KC) scheme. This support made it possible to develop and test the "Hepix" air filtration system.

References

[1] A. S. Moursi, N. El-Fishawy, S. Djahel, and M. A. Shouman, "An IoT enabled system for enhanced air quality monitoring and prediction on the edge," *Complex Intell. Syst.*, vol. 7, no. 6, pp. 2923–2947, 2021, doi: 10.1007/s40747-021-00476-w.

[2] J. Pantelic, Y. J. Son, B. Staven, and Q. Liu, "Cooking emission control with IoT sensors and connected air quality interventions for smart and healthy homes: Evaluation of effectiveness and energy consumption," *Energy Build.*, vol. 286, p. 112932, 2023, doi: 10.1016/j.enbuild.2023.112932.

[3] M. G. A. Mapili, K. A. D. Rodriguez, and J. T. Sese, "Smart Air Filtration System Using IoT and Kalman Filter Algorithm for Indoor Air Quality and Plant Monitoring," *2021 IEEE 11th Int. Conf. Syst. Eng. Technol. ICSET 2021 - Proc.*, pp. 309–314, 2021, doi: 10.1109/ICSET53708.2021.9612560.

[4] D. N. Paithankar, A. R. Pabale, R. V. Kolhe, P. William, and P. M. Yawalkar, "Framework for implementing air quality monitoring system using LPWA-based IoT technique," *Meas. Sensors*, vol. 26, no. January, p. 100709, 2023, doi: 10.1016/j.measen.2023.100709.

[5] G. Doshi and J. Stevens, "GreenAir: An IoT Field Testing System for Bio-Air Filtration," *31st Int. Conf. Comput. Theory Appl. ICCTA 2021 - Proc.*, pp. 99–103, 2021, doi: 10.1109/ICCTA54562.2021.9916633.

[6] K. Kishor and D. Pandey, "Study and Development of Efficient Air Quality Prediction System Embedded with Machine Learning and IoT," *Lect. Notes Networks Syst.*, vol. 471, pp. 313–326, 2023, doi: 10.1007/978-981-19-2535-1_24.

[7] P. William, Y. V. U. Kiran, A. Rana, D. Gangodkar, I. Khan, and K. Ashutosh, "Design and Implementation of IoT based Framework for Air Quality Sensing and Monitoring," *Proc. Int. Conf. Technol. Adv. Comput. Sci. ICTACS 2022*, pp. 197–200, 2022, doi: 10.1109/ICTACS56270.2022.9988646.

[8] M. N. M. Aashiq *et al.*, "An IoT-based handheld environmental and air quality monitoring station," *ACTA IMEKO*, vol. 12, no. 1, pp. 1–8, 2023, [Online]. Available: www.imeko.org

[9] D. Quiroga, S. Diaz, and H. F. Pastrana, "Integration of Wireless Sensor Networks and IoT for air quality monitoring," *1st IEEE Colomb. Caribb. Conf. C3 2023*, 2023, doi: 10.1109/C358072.2023.10436285.

[10] E. Dylan and A. L. Mustaram, "RUMAH POHON TAMBORA: PERBAIKAN KUALITAS UDARA MELALUI FILTRASI POLUSI UDARA PERKOTAAN DI KAWASAN TAMBORA," *STUP*, vol. 4, no. 2, pp. 2537–2544, 2022, doi: 10.24912/stupa.v4i2.

[11] D. Múnera, V. Diana, J. Aguirre, and N. G. Gómez, "IoT-based air quality monitoring systems for smart cities: A systematic mapping study," *Int. J. Electr. Comput. Eng.*, vol. 11, no. 4, pp. 3470–3482, 2021, doi: 10.11591/ijece.v11i4.pp3470-3482.

[12] M. Kamran, H. Salahuddin, I. Kashif, U. Bashir, and A. Danish, "Air Quality and Carbon Monoxide Monitoring Using IOT-based System," *J. Comput. Biomed. Informatics*, vol. 07, no. 01, 2024.

[13] W. A. Jabbar, T. Subramaniam, A. E. Ong, M. I. Shu'Ib, W. Wu, and M. A. de Oliveira, "LoRaWAN-Based IoT System Implementation for Long-Range Outdoor Air Quality Monitoring," *Internet of Things (Netherlands)*, vol. 19, no. April, p. 100540, 2022, doi: 10.1016/j.iot.2022.100540.

[14] M. Sidik and C. Ray'onaldo, "Monitoring dan Filtrasi Udara Dalam Ruangan Dengan Teknologi Plasma Berbasis IOT Dimasa New Normal," *MEANS (Media Inf. Anal. dan Sist.*, vol. 6, no. 2, pp. 101–116, 2022, doi: 10.54367/means.v6i2.1397.

[15] A. Lertsinsrubtavee, T. Kanabkaew, and S. Raksakietisak, "Detection of forest fires and pollutant plume dispersion using IoT air quality sensors," *Environ. Pollut.*, vol. 338, no. October, p. 122701, 2023, doi: 10.1016/j.envpol.2023.122701.

[16] V. Al, H. Firdaus, M. Eka, A. Nurus, and L. Aprilia, "Electrical Energy Monitoring and Analysis System At Home Using Iot-Based Prophet Algorithm," vol. 13, no. 2, pp. 1–19, 2024.

[17] L. C. Tagliabue, F. Re Cecconi, S. Rinaldi, and A. L. C. Ciribini, "Data driven indoor air quality prediction in educational facilities based on IoT network," *Energy Build.*, vol. 236, p. 110782, 2021, doi: 10.1016/j.enbuild.2021.110782.

[18] M. Iffikrul, A. Suhaidi, N. Hidayah, and M. Yunus, "Development of Blynk IoT-Based Air Quality Monitoring System," *J. Eng. Technol.*, vol. 9, no. October, pp. 63–68, 2021.

ISSN 2355-3286

Microscopic Sand Image Classification Using Convolutional Neural Networks

Christie Redja[1], Meirista Wulandari[2], Wati Asriningsih Pranoto[3]
[1,2] Department of Electrical Engineering, University Tarumanagara, Jakarta, Indonesia
[3] Department of Civil Engineering, University Tarumanagara, Jakarta, Indonesia
[1]christie.525210009@stu.untar.ac.id, [2]meiristaw@ft.untar.ac.id, [3]watip@ft.untar.ac.id

Accepted 04 December 2024
Approved 18 December 2024

***Abstract*— This research paper reviews the use of Convolutional Neural Networks (CNNs) to categorize diverse sand type using microscopic images, with an objective of improving quality control in construction materials. The paper compares three CNN architectures—LeNet-5, Inception v3, and ResNet50—for clasiffying between specific sand categories, such as two river sands (Cipongkor and Citarum) and three types of silica sand (brown, cream, and white). Each model was trained and tested on different dataset splits, with images pre-processed to highlight specific microscopic properties. To achieve a thorough comparison, each model's performance was measured using a variety of measures such as F1-score, accuracy, recall, and precision. These measurements enabled a comprehensive evaluation of how accurately and reliably each CNN model categorized the various sand types. ResNet50 consistently delivered the highest accuracy, achieving outstanding classification in some instances, accuracy 99%, showcasing its effectiveness in capturing fine details in sand textures. These results highlight the potential of CNN-based approaches for precise and automated sand classification, which supports increased quality assurance in construction and related areas.**

***Index Terms*— Convolutional Neural Network (CNN); Inception v3; LeNet-5; sand classification; ResNet50.**

I. Introduction

In recent years, the classification of materials using image-based techniques has gained significant attention due to its potential to improve accuracy and efficiency across various industries, including construction [1]. As a fundamental component in construction, sand plays a critical role in determining the quality and longevity of concrete structures. Accurate classification of different sand types is essential, as variations in sand characteristics can directly impact structural integrity. Manual sand classification methods, which rely on visual inspection and experience, are often labor-intensive, prone to human error, and lack precision [2]. Convolutional Neural Networks (CNNs) have emerged as a powerful framework for image classification due to their ability to automatically learn and extract complex visual features, enabled by advancements in machine learning and computer vision [3]. In this paper, CNNs are used to classify sand materials from microscopic images, focusing on key features such as grain texture, color variations, and morphological patterns [4]. The classification process involves two main stages: training and testing. During the training phase, the CNN model learns to identify distinctive microscopic characteristics of pre-labeled sand images, including river sand and silica sand, by progressively adjusting its weights and parameters to optimize performance. Once training is complete, the model undergoes testing using previously unseen sand images to evaluate its generalization capabilities. Metrics such as accuracy, confusion matrices, and loss values are used to assess the model's performance and reliability in practical applications.

This paper presents an automated sand classification system that employs three architectures—LeNet-5 [5], Inception v3 [6] and, ResNet50 [7] —to classify various sand types from microscopic images. The research compares the performance of these architectures in accurately distinguishing sand types, highlighting their effectiveness in enhancing material quality control in construction.

II. Research Method

A. State-of-The Art

Convolutional Neural Networks (CNNs) in sand material classification systems has been explored to analyze the recommended method against current systems. CNN has been used to classify different types of soil [8]. The research implemented a CNN-based processing module, a camera for image detection, and a dataset that included Red Soil and Black Soil. Data processing techniques applied of the Keras and TensorFlow frameworks. The Results demonstrated the model's efficacy in soil classification with a 98% accuracy rate and minimal loss values.

Deep learning and machine learning have been used to classify construction materials on unbalanced datasets [9]. In order to recognize different materials, this design applied a Vision Transformer-based processing module, a camera for image identification, and a dataset that included concrete, red bricks, and

ISSN 2355-3286

OSB boards. In this research, the Vision Transformer's performance was compared to the results of various processing modules, including Multi-Layer Perceptrons (MLPs), Support Vector Machines (SVMs), and Convolutional Neural Networks (CNNs). The results showed that, when compared to SVM and MLP, the Vision Transformer model achieved over 95% accuracy in detecting construction materials, greatly outperforming other approaches in classification accuracy.

Deep Learning: The Porosity Parameter has been applied to clasiffy soil micromorphological images [10]. Convolutional Neural Networks (CNNs) were applied to process a dataset of micromorphological soil photographs for this research. In order to increase classification accuracy of soil components based on micromorphological images, the strategy used transfer learning. The CNN model's performance was also contrasted with that of other classification techniques, including Random Forest and Support Vector Machines (SVMs). Based on measures including accuracy, precision, recall, and F1-score for each material category across three datasets, the system was able to identify soil types with 100% accuracy.

B. Block Diagram

The classification of five types of sand consist of three types of silica sand and two types of river sand. Based on their microscopic images is the focus of this research. This research comprises microscopic images of sand, including two types of river sand (Cipongkor and Citarum) and three types of silica sand (brown, cream, and white). Moreover, three CNN architectures were evaluated: ResNet50, Inception v3, and LeNet-5. The block diagram of sand classification is shown in figure 1. The block includes input, process, and output. The input is a microscopic image of sand. The process begins with detecting microscopic features of the sand using Convolutional Neural Network (CNN). The output of the system is the accuracy value of its detection and classification results of sand types. The process was simulated by using Visual Studio Code for image processing and classification.

Cipongkor and Citarum sands were specifically selected due to their prominent use in the region's construction projects. These sands are valued for their smooth texture, uniform grain size, and excellent durability, which contribute to superior performance in concrete and mortar applications. As they are frequently utilized in local construction practices, their inclusion in the dataset ensures the research relevance to real-world applications, particularly in addressing quality control challenges for commonly used materials in the area.

LeNet-5, Inception v3, and ResNet50 were selected for their various design approaches and ability to handle varying levels of image complexity and details. LeNet-5, a core CNN model, served as a baseline for evaluating the effectiveness of early CNN architectures in sand classification. Inception v3, known for its multi-scale feature extraction enabled by modified convolutions, was chosen to investigate its efficacy on textures with considerable variability. ResNet50, which incorporates residual learning and a deep architecture, was chosen to investigate its capacity to recognize complicated picture features while addressing training issues such as vanishing gradients. The integration of these models results in a full evaluation of sand classification performance across various CNN configurations.

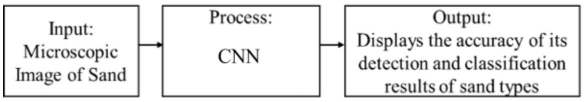

Fig. 1. Block Diagram of Sand Material Classification System

C. Digital Microscope Camera

The digital microscope camera is a camera to capture high-resolution images of specimens under magnification and display them on a computer or monitor. It enables real-time and detailed observation of microscopic samples, enhancing both viewing and analysis processes [11]. In this paper, the digital microscope camera capture microscopic images of sand particles as the input data for the Convolutional Neural Network (CNN) model. These images provide detailed representations of the sand's texture and morphology, enabling the CNN to learn and classify various sand types based on their unique microstructural properties. The digital microscope camera is illustrated in Figure 2.

Fig. 2. Digital Microscope Camera

D. Sand Materials

Sand is a common granular material in construction, composed of small rock and mineral particles with diameters ranging from 0.0625 mm to 2 mm [12]. In this paper, two types of river sand and three types of silica sand were used as the dataset. River sand, originating from riverbeds, consists of rounded particles shaped by natural erosion and transportation. Its smooth texture and high quality make it ideal for applications in concrete and mortar [13]. In contrast, silica sand, primarily composed of silicon dioxide (SiO_2), is valued for its chemical resistance and hardness. Due to its purity and durability, silica sand is widely used in industries such as hydraulic fracturing, foundry casting, and glassmaking [14]. Images of the sand material used as a dataset can be seen at Figure 3.

Fig. 3. Image Dataset: (a) Cipongkor River Sand, (b) Sand Citarum River, (c) Cream Silica Sand, (d) Brown Silica Sand, (e) White Silica Sand

E. *Convolutional Neural Network (CNN)*

A Convolutional Neural Network (CNN) is a deep learning architecture designed to process and recognize patterns in image data through hierarchical layers. CNNs are particularly effective for image classification tasks because they can automatically extract and learn features from raw pixel data without requiring manual feature selection. The structure of CNNs is inspired by the visual processing mechanisms of biological systems, specifically the hierarchical pattern recognition of the human brain [15] . The example of CNN structure is shown in Figure 4.

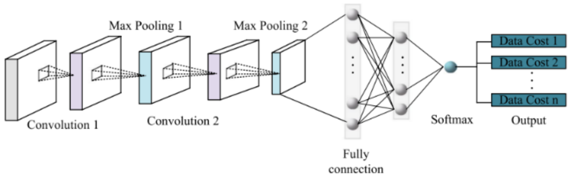

Fig. 4. Structure of a Convolutional Neural Network for Image Classification [15]

CNNs consist of several types of layers, each playing a key role in the network's ability to process image data:

- Convolutional Layer: This is the first layer where filters (kernels) are applied to the input image. Each filter slides across the image to capture low-level features like edges, textures, and colors. The result is a set of feature maps that represent different aspects of the input data. These feature maps serve as the foundation for deeper layers to learn more complex patterns.
- Activation Layer: Activation functions are applied following convolutional processes to introduce non-linearity into the network. Functions like Rectified Linear Units (ReLU) help the network capture complex, non-linear relationships within the data.
- Pooling Layer**:** The pooling layer reduces the dimensionality of feature maps while retaining key information. Max-pooling, a common technique, captures the peak value within a specific window, reducing feature map size and aiding in overfitting prevention.
- Batch Normalization Layer**:** This layer normalizes the input to each layer, helping to stabilize the learning process and speed up training. Batch normalization ensures that the network remains robust by preventing large variations in the input data.
- Dropout Layer**:** Dropout is a method for decreasing overfitting in which some neurons are randomly "ignored" during training. This forces the network to create more robust and redundant feature sets.
- Fully Connected Layer**:** The feature maps are flattened into a single vector and routed through one or more completely connected layers. This layer outputs the classification probabilities or the predicted labels for the input image, depending on the problem [16].

These CNN models are optimized to detect the minor differences in texture, coloration, and shape of grains that characterize each sand type. A comparison of sand classification performance is conducted using three prominent CNN architectures, LeNet-5 [5], Inception v3 [6] and, ResNet50 [7].

1) *LeNet-5*

LeNet-5, introduced by Yann LeCun in the late 1990s, was initially designed for image recognition tasks, specifically for classifying handwritten digits [5]. LeNet-5 is a convolutional neural network (CNN) architecture based on gradient descent, originally developed for recognizing handwritten digits. An input layer that processes 32×32 pixel pictures of digits (0–9) and an output layer with 10 nodes, each of which corresponds to a digit from 0–9, make up the conventional LeNet-5 design shown in Figure 5. Three convolutional layers, two pooling layers, and one fully connected layer make up LeNet-5's six extra layers in addition to the input and output layers. A 2×2 kernel is used by the pooling layers, and 5×5 filters are applied by the convolutional layers. Additionally, the fully linked layer lowers the number of neurons from 120 to 84, improving the model's parameter training efficiency [17]. However, its architecture is also effective at classifying patterns and textures in different images, making it useful for tasks like sand classification, where detecting microstructural details is important.

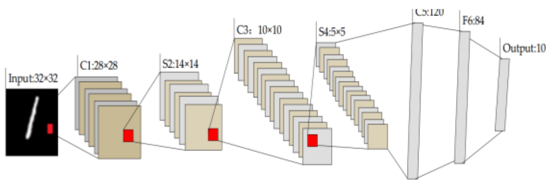

Fig. 5. LeNet-5 Architecture [18]

2) *Inception v3*

Inception v3 is a convolutional neural network (CNN) architecture developed by Google for efficient image classification tasks. The primary novelty of Inception v3 is its capacity to extract both fine and larger details from an image by employing several filter sizes (1×1, 3×3, 5×5) to collect multi-scale characteristics within the same layer [6]. This approach makes Inception v3 highly effective in handling complex images where the object size and features can vary significantly.

One of the primary improvements in Inception v3 is the use of factorized convolutions, which break down larger convolutions into smaller ones (e.g., 3×3 into two 1×3 and 3×1 convolutions). This increases computational performance and lowers the number of parameters without compromising accuracy. To stabilize the learning process and speed up and improve the reliability of training, the model also includes batch normalization [19]. The model's architecture is presented in Figure 6.

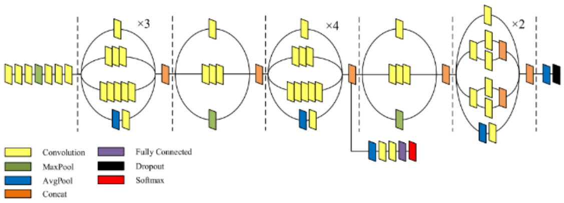

Fig. 6. Inception v3 network structure [19]

In this paper, Inception v3 is used to classify microscopic images of sand, classifying different types of sand grains based on their textures and microstructures. The architecture's ability to handle varying scales and extract detailed features makes it well-suited for this task, as the sand grains exhibit diverse shapes and patterns that require robust feature extraction for accurate classification.

3) ResNet50 (Residual Networks)

ResNet50 is a deep convolutional neural network (CNN) architecture developed to address the vanishing gradient issue that often occurs in extremely deep networks. ResNet incorporates shortcut connections that bypass certain layers, facilitating residual learning. This approach allows layers to capture the difference, or residual, between the input and the target output [7]. These connections facilitate the retention of information within the network and simplify the training process. The 50 layers of the ResNet50 model are composed of convolutional layers followed by identity shortcuts in each residual block. This architecture ensures efficient learning by allowing layers to focus on the residuals, improving accuracy and enabling deeper networks to perform better without degradation in training [20]. The structure of ResNet50 is illustrated in Figure 7.

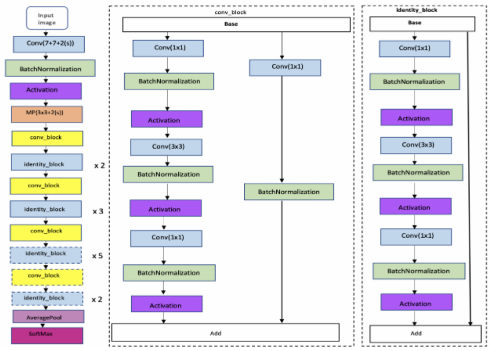

Fig. 7. Architecture of ResNet50 [20]

In this system, ResNet50 is applied to classify sand images by detecting subtle microstructural patterns in sand grains. The residual connections allow the model to capture and generalize complex features across different types of sand, improving classification accuracy.

F. Confusion Matrix

A confusion matrix is an important tool for assessing the effectiveness of a classification model [19]. It presents a clear overview of the model's predictions in comparison to the actual ground truth, classifying the outcomes into four distinct situations:

- True Positive (TP): Both the predicted and actual classes are implied to be positive since the model accurately predicts the positive class.
- The True Negative (TN): Both the predicted and actual classes are negative, demonstrating that the model effectively recognizes the negative class.
- False Positive (FP): The model makes a mistake when it predicts the positive class when the real class is negative.
- False Negative (FN): When the model wrongly assigns a positive instance to the negative class. [21].

The confusion matrix is especially useful in multi-class classification tasks, like the sand classification in this paper, as it highlights how well the model distinguishes between different classes. Key metrics including accuracy, precision, recall, and F1-score can be obtained by examining the confusion matrix; this gives information about the model's advantages and shortcomings.

In this paper, confusion matrices are constructed for LeNet-5 [5], Inception v3 [6] and, ResNet50 [7]. models to evaluate their performance in classifying different sand types. The confusion matrix supports to classify patterns of misclassification, assess the model's reliability, and guide further optimization.

Model accuracy, a standard metric obtained from the confusion matrix, is determined by calculating the proportion of correctly predicted cases (including both true positives and true negatives) relative to the total instances in the dataset. The formula to calculate accuracy is as follows.The formula for accuracy is as follows:

$$Accuracy = \frac{TP + TN}{TP + TN + FP + FN} \qquad (1)$$

- **TP** = True Positives (correctly predicted positive cases)
- **TN** = True Negatives (correctly predicted negative cases)
- **FP** = False Positives (incorrectly predicted positive cases)
- **FN** = False Negatives (incorrectly predicted negative cases) [22]

III. Results and Discussion

A. Results

The dataset used in this paper contains 150 images for each sand type, including two river sand types (Cipongkor and Citarum) and three silica sand types (brown, cream, and white). The total amount of data is 750 images for 5 types of sand. The images were captured using a high-resolution digital microscope and were resized into 150×150 pixel as the input for CNN.

The dataset was split into five different ratios: 70:30, 75:25, 80:20, 85:15, and 90:10, with percentages allocated to training and testing sets, respectively. Exploring different training and testing data splits in this research was essential to obtain the optimum model's performance. This suggests an excellent convergence between generalization and learning, improving classification results. For each ratio, the training set contained train data and validation data. The train data consist of the majority of the images to ensure the models had sufficient data to learn and validation data were used to fine-tune the models. Test set was used to evaluate model performance. While the dataset provides a solid foundation for a preliminary research, its particular focus on specific sand samples may limit ability to generalize and cause overfitting issues. To address these issues, data augmentation methods such as random rotations, width and height shifts, zooming, brightness adjustments, and horizontal flipping were used to increase the dataset's diversity and reduce overfitting.

We compare three CNN models—LeNet-5, Inception v3, and ResNet50—optimized to distinguish fine-grained properties of sand types, including as texture, coloring, and morphology. To ensure uniform evaluation, all models were trained with the Adam optimizer, learning rate 0.00001, a batch size of 32, and up to 100 epochs. The comparison of accuracy across different dataset splits for LeNet-5 [5], Inception V3 [6], and ResNet50 [7] models is presented in Table I.

TABLE I. Accuracy Comparison Of Different Models Across Dataset Splitsable Styles

Dataset Split	CNN Architectures Accuracy		
	***LeNet-5* [5]**	***Inception v3* [6]**	***ResNet50* [7]**
70 : 30	59%	93%	93%
75 : 25	45%	96%	97%
80 : 20	72%	92%	92%
85 : 15	43%	92%	99%
90 : 10	70%	95%	95%

Table I presents a comparison of accuracy among three CNN architectures LeNet-5 [5], Inception v3 [6], and ResNet50 [7] across different dataset splits. LeNet-5 demonstrates the lowest performance among the models, with its highest accuracy recorded at 72% in the 80:20 split. Inception v3 performs considerably better, maintaining an accuracy of over 92% in the majority of splits. However, ResNet50 consistently outperforms both, achieving outstanding classification accuracy (upto 100%) at the 85:15 split. ResNet50 showed the superior performance results based on its capacity to apply residual learning in maintaining accuracy over deeper layers, which allows it to capture subtle microstructural differences in the sand images. The results exceed those reported in previous research, offering a benchmark for novelty and validating the effectiveness of the proposed approach.

Although the primary parameter to evaluate the model's classification performance was accuracy, other metrics such as F1-score, precision, recall, and confusion matrix were also employed to obtain a more comprehensive understanding of how well the model performed. Figure 8 shows the confusion matrix for the LeNet-5 model, Figure 9 illustrates the results for Inception v3, and Figure 10 displays the matrix for ResNet50. These matrices provide a detailed view of how each model classified the different sand types.To gain deeper insights into the classification performance, confusion matrices for each architecture are presented. Figure 8 shows the confusion matrix for the LeNet-5 model, Figure 9 illustrates the results for Inception v3, and Figure 10 displays the matrix for ResNet50. These matrices provide a detailed view of how each model classified the different sand types.

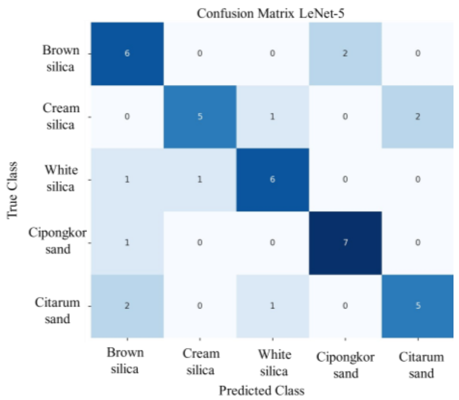

Fig. 8. Confusion Matrix for LeNet-5 Model in Sand Type Classification

From the confusion matrix, it is evident that the model achieves its best performance when classifying Cipongkor sand and Brown silica, as both sand types are correctly classified in most instances. The model shows strong accuracy in detecting these two categories, which have clear distinguishing features.

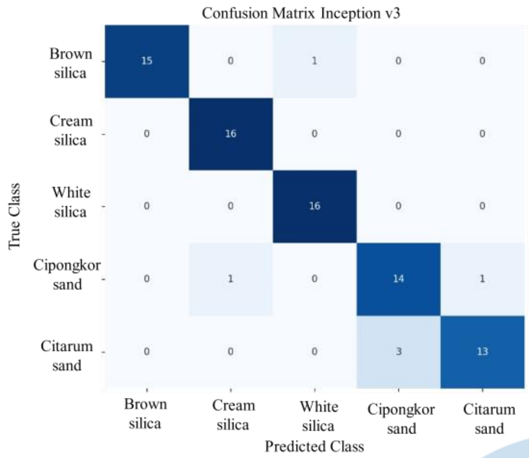

Fig. 9. Matrix for Inception v3 Model in Sand Type Classification

From the confusion matrix, the model achieves near-perfect classification for Brown silica, Cream silica, and White silica, as indicated by the diagonal dominance in the confusion matrix. The true positive rates for these sand types are impressive, showing the model's effectiveness in capturing the unique characteristics of these specific sand types.

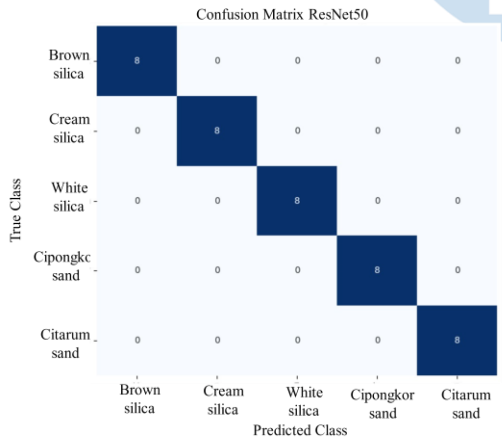

Fig. 10. Confusion Matrix for ResNet50 Model in Sand Type Classification

From the confusion matrix, we can observe that the model classifies all sand types with 100% accuracy. The matrix shows no misclassifications, indicating that the model effectively classifies each of the five sand types with complete precision, ensuring flawless performance in recognizing microscopic features.

Following the analysis of the confusion matrices, it is crucial to evaluate the models using more detailed performance metrics such as precision, recall, and F1-scores. These metrics provide a deeper understanding of how effectively each CNN architecture classifies various sand types [23]. While accuracy offers a general overview, precision, recall, and F1-scores give more specific insights into the balance between true positives, false positives, and false negatives within the classification outcomes.

Tables II, III, and IV present the precisions, recalls, and F1-scores for LeNet-5, Inception v3, and ResNet50, respectively, demonstrating each model's performance across different sand classification tasks.

TABLE II. LENET-5 RESULT

Class	Precision	Recall	F1-Score
Brown silica	0.6	0.75	0.67
Cream silica	0.83	0.62	0.71
White silica	0.75	0.75	0.75
Cipongkor sand	0.78	0.88	0.82
Citarum sand	0.71	0.62	0.67

Based on Table II, Cipongkor sand achieved the best performance with an F1-score of 0.82, while White silica also performed well with an F1-score of 0.75. Cream silica had the highest precision (0.83) but lower recall, resulting in an F1-score of 0.71. Brown silica and Citarum sand had lower F1-scores, both at 0.67, indicating areas where classification could be improved.

TABLE III. INCEPTION V3 RESULT

Class	Precision	Recall	F1-Score
Brown silica	1.0	0.94	0.97
Cream silica	0.94	1.0	0.97
White silica	0.94	1.0	0.97
Cipongkor sand	0.82	0.88	0.85
Citarum sand	0.93	0.81	0.87

Based on Table III, Inception v3 demonstrates high performance, with Brown silica, Cream silica, and White silica achieving F1-scores of 0.97. Cipongkor sand and Citarum sand, while slightly lower, still perform well with F1-scores of 0.85 and 0.87, respectively, indicating strong classification capabilities for all sand types.

TABLE IV. RESNET50 RESULT

Class	Precision	Recall	F1-Score
Brown silica	1.0	1.0	1.0
Cream silica	1.0	1.0	1.0
White silica	1.0	1.0	1.0
Cipongkor sand	1.0	1.0	1.0
Citarum sand	1.0	1.0	1.0

As shown in Table IV, ResNet50 achieves perfect results, with all sand types having precision, recall, and F1-scores of 1.0. This indicates that ResNet50 classifies all sand types flawlessly without any misclassifications.

IV. CONCLUSION

In this paper, sand type classification was performed using three Convolutional Neural Network (CNN) architectures—LeNet-5, Inception v3, and ResNet50—

on microscopic images to determine accuracy in distinguishing between sand types. Based on the results, LeNet-5 and Inception v3 both demonstrated strong performance in classifying sand types, showing their effectiveness for image processing tasks. However, ResNet50 consistently achieved the highest accuracy across all dataset splits, making it the most effective model for this research.

The results highlight the potential of CNN-based systems in real-world applications, such as material quality inspection in the construction industry. Using these models in automated systems alongside digital microscope cameras could offer a dependable solution for fast and accurate analyzing sand samples, obtaining the demands of industries such as concrete production.This approach minimizes human error, reduces inspection time, and improves the consistency of material quality, ultimately enhancing the durability and reliability of construction projects.

Nevertheless, this paper has limitations, including the use of a relatively small dataset and specific sand types, which may impact the generalizability of the models. Further research should focus on expanding the dataset to include a wider range of sand types and conditions while exploring additional CNN architectures and techniques to further improve classification accuracy. These steps will ensure the robustness and applicability of the proposed models in broader industrial contexts.

Acknowledgment

The author would like to express sincere gratitude to Lembaga Penelitian dan Pengabdian kepada Masyarakat (LPPM) Universitas Tarumanagara and Electrical Engineering Department, Faculty of Engineering, Universitas Tarumanagara.

References

[1] K. Mostafa and T. Hegazy, "Review of image-based analysis and applications in construction," Feb. 01, 2021, *Elsevier B.V.* doi: 10.1016/j.autcon.2020.103516.

[2] C. Y. Liu, C. Y. Ku, T. Y. Wu, and Y. C. Ku, "An Advanced Soil Classification Method Employing the Random Forest Technique in Machine Learning," *Applied Sciences (Switzerland)*, vol. 14, no. 16, Aug. 2024, doi: 10.3390/app14167202.

[3] L. Chen, S. Li, Q. Bai, J. Yang, S. Jiang, and Y. Miao, "Review of image classification algorithms based on convolutional neural networks," Nov. 01, 2021, *MDPI*. doi: 10.3390/rs13224712.

[4] O. Nitin Shendge, N. Kumar Singh, and K. Naaz, "Classification Of All-Purpose Sand: A Deep Learning Approach," Pune, India: Proceedings of WRFER International Conference, May 2023.

[5] L. Alzubaidi *et al.*, "Review of deep learning: concepts, CNN architectures, challenges, applications, future directions," *J Big Data*, vol. 8, no. 1, Dec. 2021, doi: 10.1186/s40537-021-00444-8.

[6] A. E. Minarno, L. Aripa, Y. Azhar, and Y. Munarko, "Classification of Malaria Cell Image Using Inception-V3 Architecture," *INTERNATIONAL JOURNAL ON INFORMATICS VISUALIZATION*, pp. 273–278, Jun. 2023, [Online]. Available: www.joiv.org/index.php/joiv

[7] E. Suherman, B. Rahman, D. Hindarto, and H. Santoso, "Implementation of ResNet-50 on End-to-End Object Detection (DETR) on Objects," *SinkrOn*, vol. 8, no. 2, pp. 1085–1096, Apr. 2023, doi: 10.33395/sinkron.v8i2.12378.

[8] C. Author, A. David Ronaldo, U. Respati Yogyakarta, U. Respati Yogyakarta hamzah, and M. Diqi, "Effective Soil Type Classification Using Convolutional Neural Network," *International Journal of Informatics and Computation (IJICOM)*, vol. 3, no. 1, 2021, doi: 10.35842/ijicom.

[9] M. Soleymani, M. Bonyani, H. Mahami, and F. Nasirzadeh, "Construction material classification on imbalanced datasets using vision transformer (ViT) architecture," *arXiv preprint arXiv:2108.09527*, 2021.

[10] R. Arnay, J. Hernández-Aceituno, and C. Mallol, "Soil micromorphological image classification using deep learning: The porosity parameter," *Appl Soft Comput*, vol. 102, Apr. 2021, doi: 10.1016/j.asoc.2021.107093.

[11] M. Harfouche *et al.*, "Imaging across multiple spatial scales with the multi-camera array microscope," Nov. 2022, [Online]. Available: http://arxiv.org/abs/2212.00027

[12] B. Wang, S. Xin, D. Jin, L. Zhang, J. Wu, and H. Guo, "A New Porosity Evaluation Method Based on a Statistical Methodology for Granular Material: A Case Study in Construction Sand," *Applied Sciences (Switzerland)*, vol. 14, no. 16, Aug. 2024, doi: 10.3390/app14167379.

[13] M. W. M. Abdias, M. M. Blanche, U. J. P. Nana, H. F. Abanda, N. François, and P. Chrispin, "River Sand Characterization for Its Use in Concrete: A Revue," *Open Journal of Civil Engineering*, vol. 13, no. 02, pp. 353–366, 2023, doi: 10.4236/ojce.2023.132027.

[14] U. Okereafor, M. Makhatha, L. Mekuto, and V. Mavumengwana, "Gold mine tailings: A potential source of silica sand for glass making," *Minerals*, vol. 10, no. 5, May 2020, doi: 10.3390/min10050448.

[15] X. Zhao, L. Wang, Y. Zhang, X. Han, M. Deveci, and M. Parmar, "A review of convolutional neural networks in computer vision," *Artif Intell Rev*, vol. 57, no. 4, Apr. 2024, doi: 10.1007/s10462-024-10721-6.

[16] A. Zafar *et al.*, "Convolutional Neural Networks: A Comprehensive Evaluation and Benchmarking of Pooling Layer Variants," *Symmetry (Basel)*, vol. 16, no. 11, Nov. 2024, doi: 10.3390/sym16111516.

[17] G. Wei, G. Li, J. Zhao, and A. He, "Development of a LeNet-5 gas identification CNN structure for electronic noses," *Sensors (Switzerland)*, vol. 19, no. 1, Jan. 2019, doi: 10.3390/s19010217.

[18] L. Wan, Y. Chen, H. Li, and C. Li, "Rolling-element bearing fault diagnosis using improved lenet-5 network," *Sensors (Switzerland)*, vol. 20, no. 6, Mar. 2020, doi: 10.3390/s20061693.

[19] N. Dong, L. Zhao, C. H. Wu, and J. F. Chang, "Inception v3 based cervical cell classification combined with artificially extracted features," *Appl Soft Comput*, vol. 93, Aug. 2020, doi: 10.1016/j.asoc.2020.106311.

[20] B. Mandal, A. Okeukwu, and Y. Theis, "Masked Face Recognition using ResNet-50," Apr. 2021, [Online]. Available: http://arxiv.org/abs/2104.08997

[21] D. Bhisetya Rarasati, "Recommendation for Classification of News Categories Using Support Vector Machine Algorithm with SVD," *Ultimatics : Jurnal Teknik Informatika*, vol. 13, no. 2, p. 72, 2021, [Online]. Available: www.waspada.com,

[22] M. Widjaja and A. Suryadibrata, "Comparison of Fine-tuned CNN Architectures for COVID-19 Infection Diagnosis," *Ultimatics : Jurnal Teknik Informatika*, vol. 16, no. 1, p. 63, 2024.

[23] M. Naufal, A. Saputro, F. Liantoni, and D. Maryono, "Application of Convolutional Neural Network (CNN) Using TensorFlow as a Learning Medium for Spice Classification," *Ultimatics : Jurnal Teknik Informatika*, vol. 16, no. 1, 2024.

AUTHOR GUIDELINES

1. Manuscript criteria

- The article has never been published or in the submission process on other publications.
- Submitted articles could be original research articles or technical notes.
- The similarity score from plagiarism checker software such as Turnitin is 20% maximum.
- For December 2021 publication onwards, Ultima Computing : Jurnal Sistem Komputer will be receiving and publishing manuscripts written in English only.

2. Manuscript format

- Article been type in Microsoft Word version 2007 or later.
- Article been typed with 1 line spacing on an A4 paper size (21 cm x 29,7 cm), top-left margin are 3 cm and bottom-right margin are 2 cm, and Times New Roman's font type.
- Article should be prepared according to the following author guidelines in this template. Article contain of minimum 3500 words.
- References contain of minimum 15 references (primary references) from reputable journals/conferences

3. Organization of submitted article

The organization of the submitted article consists of Title, Abstract, Index Terms, Introduction, Method, Result and Discussion, Conclusion, Appendix (if any), Acknowledgment (if any), and References.

- Title
  The maximum words count on the title is 12 words (including the subtitle if available)
- Abstract
  Abstract consists of 150-250 words. The abstract should contain logical argumentation of the research taken, problem-solving methodology, research results, and a brief conclusion.
- Index terms
  A list in alphabetical order in between 4 to 6 words or short phrases separated by a semicolon (;), excluding words used in the title and chosen carefully to reflect the precise content of the paper.
- Introduction
  Introduction commonly contains the background, purpose of the research, problem identification, research methodology, and state of the art conducted by the authors which describe implicitly.
- Method
  Include sufficient details for the work to be repeated. Where specific equipment and materials are named, the manufacturer's details (name, city and country) should be given so that readers can trace specifications by contacting the manufacturer. Where commercially available software has been used, details of the supplier should be given in brackets or the reference given in full in the reference list.
- Results and Discussion
  State the results of experimental or modeling work, drawing attention to important details in tables and figures, and discuss them intensively by comparing and/or citing other references.
- Conclusion
  Explicitly describes the research's results been taken. Future works or suggestion could be explained after it
- Appendix and acknowledgment, if available, could be placed after Conclusion.
- All citations in the article should be written on References consecutively based on its' appearance order in the article using Mendeley (recommendation). The typing format will be in the same format as the IEEE journals and transaction format.

4. Reviewing of Manuscripts

Every submitted paper is independently and blindly reviewed by at least two peer-reviewers. The decision for publication, amendment, or rejection is based upon their reports/recommendations. If two or more reviewers consider a manuscript unsuitable for publication in this journal, a statement explaining the basis for the decision will be sent to the authors within six months of the submission date.

5. Revision of Manuscripts

Manuscripts sent back to the authors for revision should be returned to the editor without delay (maximum of two weeks). Revised manuscripts can be sent to the editorial office through the same online system. Revised manuscripts returned later than one month will be considered as new submissions.

6. Editing References

- **Periodicals**
  J.K. Author, "Name of paper," Abbrev. Title of Periodical, vol. x, no. x, pp. xxx-xxx, Sept. 2013.

- **Book**
  J.K. Author, "Title of chapter in the book," in Title of His Published Book, xth ed. City of Publisher, Country or Nation: Abbrev. Of Publisher, year, ch. x, sec. x, pp xxx-xxx.

- **Report**
  J.K. Author, "Title of report," Abbrev. Name of Co., City of Co., Abbrev. State, Rep. xxx, year.

- **Handbook**
  Name of Manual/ Handbook, x ed., Abbrev. Name of Co., City of Co., Abbrev. State, year, pp. xxx-xxx.

- **Published Conference Proceedings**
  J.K. Author, "Title of paper," in Unabbreviated Name of Conf., City of Conf., Abbrev. State (if given), year, pp. xxx-xxx.

- **Papers Presented at Conferences**
  J.K. Author, "Title of paper," presented at the Unabbrev. Name of Conf., City of Conf., Abbrev. State, year.

- **Patents**
  J.K. Author, "Title of patent," US. Patent xxxxxxx, Abbrev. 01 January 2014.

- **Theses and Dissertations**
  J.K. Author, "Title of thesis," M.Sc. thesis, Abbrev. Dept., Abbrev. Univ., City of Univ., Abbrev. State, year. J.K. Author, "Title of dissertation," Ph.D. dissertation, Abbrev. Dept., Abbrev. Univ., City of Univ., Abbrev. State, year.

- **Unpublished**
  J.K. Author, "Title of paper," unpublished. J.K. Author, "Title of paper," Abbrev. Title of Journal, in press.

- **On-line Sources**
  J.K. Author. (year, month day). Title (edition) [Type of medium]. Available: http:// www.(URL) J.K. Author. (year, month). Title. Journal [Type of medium]. volume(issue), pp. if given. Available: http://www.(URL) Note: type of medium could be online media, CD-ROM, USB, etc.

7. Editorial Adress

Jl. Scientia Boulevard, Gading Serpong
Tangerang, Banten, 15811
Email: **ultimacomputing@umn.ac.id**

Paper Title

Subtitle (if needed)

Author 1 Name[1], Author 2 Name[2], Author 3 Name[2]
[1] Line 1 (of affiliation): dept. name of organization, organization name, City, Country
Line 2: e-mail address if desired
[2] Line 1 (of affiliation): dept. name of organization, organization name, City, Country
Line 2: e-mail address if desired

Accepted on mmmmm dd, yyyy
Approved on mmmmm dd, yyyy

***Abstract*—This electronic document is a "live" template which you can use on preparing your Ultima Computing paper. Use this document as a template if you are using Microsoft Word 2007 or later. Otherwise, use this document as an instruction set. Do not use symbol, special characters, or Math in Paper Title and Abstract. Do not cite references in the abstract.**

***Index Terms*—enter key words or phrases in alphabetical order, separated by semicolon (;)**

I. Introduction

This template, modified in MS Word 2007 and saved as a Word 97-2003 document, provides authors with most of the formatting specifications needed for preparing electronic versions of their papers. Margins, column widths, line spacing, and type styles are built-in here. The authors must make sure that their paper has fulfilled all the formatting stated here.

Introduction commonly contains the background, purpose of the research, problem identification, and research methodology conducted by the authors which been describe implicitly. Except for Introduction and Conclusion, other chapter's title must be explicitly represent the content of the chapter.

II. Ease of Use

A. Selecting a Template

First, confirm that you have the correct template for your paper size. This template is for Ultima Computing. It has been tailored for output on the A4 paper size.

B. Maintaining the Integrity of the Specifications

The template is used to format your paper and style the text. All margins, column widths, line spaces, and text fonts are prescribed; please do not alter them.

III. Prepare Your Paper Before Styling

Before you begin to format your paper, first write and save the content as a separate text file. Keep your text and graphic files separate until after the text has been formatted and styled. Do not add any kind of pagination anywhere in the paper. Please take note of the following items when proofreading spelling and grammar.

A. Abbreviations and Acronyms

Define abbreviations and acronyms the first time they are used in the text, even after they have been defined in the abstract. Abbreviations such as IEEE, SI, MKS, CGS, sc, dc, and rms do not have to be defined. Abbreviations that incorporate periods should not have spaces: write "C.N.R.S.," not "C. N. R. S." Do not use abbreviations in the title or heads unless they are unavoidable.

B. Units

- Use either SI (MKS) or CGS as primary units (SI units are encouraged).
- Do not mix complete spellings and abbreviations of units: "Wb/m2" or "webers per square meter," not "webers/m2." Spell units when they appear in text: "...a few henries," not "...a few H."
- Use a zero before decimal points: "0.25," not ".25."

C. Equations

The equations are an exception to the prescribed specifications of this template. You will need to determine whether or not your equation should be typed using either the Times New Roman or the Symbol font (please no other font). To create multileveled equations, it may be necessary to treat the equation as a graphic and insert it into the text after your paper is styled.

Number the equations consecutively. Equation numbers, within parentheses, are to position flush right, as in (1), using a right tab stop.

$$\int_0^{r_2} F(r,\phi)\, dr\, d\phi = [\sigma r_2 / (2\mu_0)] \tag{1}$$

Note that the equation is centered using a center tab stop. Be sure that the symbols in your equation have been defined before or immediately following the equation. Use “(1),” not “Eq. (1)” or “equation (1),” except at the beginning of a sentence: “Equation (1) is ...”

D. Some Common Mistakes

- The word “data” is plural, not singular.
- The subscript for the permeability of vacuum μ_0, and other common scientific constants, is zero with subscript formatting, not a lowercase letter “o.”
- In American English, commas, semi-/colons, periods, question and exclamation marks are located within quotation marks only when a complete thought or name is cited, such as a title or full quotation. When quotation marks are used, instead of a bold or italic typeface, to highlight a word or phrase, punctuation should appear outside of the quotation marks. A parenthetical phrase or statement at the end of a sentence is punctuated outside of the closing parenthesis (like this). (A parenthetical sentence is punctuated within the parentheses.)
- A graph within a graph is an “inset,” not an “insert.” The word alternatively is preferred to the word “alternately” (unless you really mean something that alternates).
- Do not use the word “essentially” to mean “approximately” or “effectively.”
- In your paper title, if the words “that uses” can accurately replace the word using, capitalize the “u”; if not, keep using lower-cased.
- Be aware of the different meanings of the homophones “affect” and “effect,” “complement” and “compliment,” “discreet” and “discrete,” “principal” and “principle.”
- Do not confuse “imply” and “infer.”
- The prefix “non” is not a word; it should be joined to the word it modifies, usually without a hyphen.
- There is no period after the “et” in the Latin abbreviation “et al.”
- The abbreviation “i.e.” means “that is,” and the abbreviation “e.g.” means “for example.”

IV. Using the Template

After the text edit has been completed, the paper is ready for the template. Duplicate the template file by using the Save As command, and use the naming convention as below

ULTIMATICS_firstAuthorName_paperTitle.

In this newly created file, highlight all of the contents and import your prepared text file. You are now ready to style your paper. Please take note on the following items.

A. Authors and Affiliations

The template is designed so that author affiliations are not repeated each time for multiple authors of the same affiliation. Please keep your affiliations as succinct as possible (for example, do not differentiate among departments of the same organization).

B. Identify the Headings

Headings, or heads, are organizational devices that guide the reader through your paper. There are two types: component heads and text heads.

Component heads identify the different components of your paper and are not topically subordinate to each other. Examples include ACKNOWLEDGMENTS and REFERENCES, and for these, the correct style to use is “Heading 5.”

Text heads organize the topics on a relational, hierarchical basis. For example, the paper title is the primary text head because all subsequent material relates and elaborates on this one topic. If there are two or more sub-topics, the next level head (uppercase Roman numerals) should be used and, conversely, if there are not at least two sub-topics, then no subheads should be introduced. Styles, named “Heading 1,” “Heading 2,” “Heading 3,” and “Heading 4”, are prescribed.

C. Figures and Tables

Place figures and tables at the top and bottom of columns. Avoid placing them in the middle of columns. Large figures and tables may span across both columns. Figure captions should be below the figures; table heads should appear above the tables. Insert figures and tables after they are cited in the text. Use the abbreviation “Fig. 1,” even at the beginning of a sentence.

TABLE I. TABLE STYLES

Table Head	**Table Column Head**		
	Table column subhead	***Subhead***	***Subhead***
copy	More table copy		

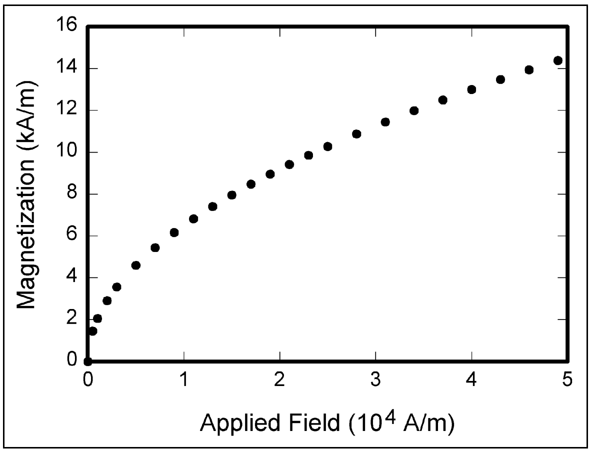

Fig. 1. Example of a figure caption

V. Conclusion

A conclusion section is not required. Although a conclusion may review the main points of the paper, do not replicate the abstract as the conclusion. A conclusion might elaborate on the importance of the work or suggest applications and extensions.

Appendix

Appendixes, if needed, appear before the acknowledgment.

ACKNOWLEDGMENT

The preferred spelling of the word "acknowledgment" in American English is without an "e" after the "g." Use the singular heading even if you have many acknowledgments. Avoid expressions such as "One of us (S.B.A.) would like to thank ... ." Instead, write "F. A. Author thanks ... ." You could also state the sponsor and financial support acknowledgments here.

References

The template will number citations consecutively within brackets [1]. The sentence punctuation follows the bracket [2]. Refer simply to the reference number, as in [3]—do not use "Ref. [3]" or "reference [3]" except at the beginning of a sentence: "Reference [3] was the first ..."

Number footnotes separately in superscripts. Place the actual footnote at the bottom of the column in which it was cited. Do not put footnotes in the reference list. Use letters for table footnotes.

Unless there are six authors or more give all authors' names; do not use "et al.". Papers that have not been published, even if they have been submitted for publication, should be cited as "unpublished" [4]. Papers that have been accepted for publication should be cited as "in press" [5]. Capitalize only the first word in a paper title, except for proper nouns and element symbols.

For papers published in translation journals, please give the English citation first, followed by the original foreign-language citation [6].

[1] G. Eason, B. Noble, and I.N. Sneddon, "On certain integrals of Lipschitz-Hankel type involving products of Bessel functions," Phil. Trans. Roy. Soc. London, vol. A247, pp. 529-551, April 1955. (*references*)

[2] J. Clerk Maxwell, A Treatise on Electricity and Magnetism, 3rd ed., vol. 2. Oxford: Clarendon, 1892, pp.68-73.

[3] I.S. Jacobs and C.P. Bean, "Fine particles, thin films and exchange anisotropy," in Magnetism, vol. III, G.T. Rado and H. Suhl, Eds. New York: Academic, 1963, pp. 271-350.

[4] K. Elissa, "Title of paper if known," unpublished.

[5] R. Nicole, "Title of paper with only first word capitalized," J. Name Stand. Abbrev., in press.

[6] Y. Yorozu, M. Hirano, K. Oka, and Y. Tagawa, "Electron spectroscopy studies on magneto-optical media and plastic substrate interface," IEEE Transl. J. Magn. Japan, vol. 2, pp. 740-741, August 1987 [Digests 9th Annual Conf. Magnetics Japan, p. 301, 1982].

[7] M. Young, The Technical Writer's Handbook. Mill Valley, CA: University Science, 1989.

UMN

UNIVERSITAS MULTIMEDIA NUSANTARA

ISSN 2355-3286

9 772355 328009

UMN
UNIVERSITAS
MULTIMEDIA
NUSANTARA

PRESS

Universitas Multimedia Nusantara
Scientia Garden Jl. Boulevard Gading Serpong, Tangerang
Telp. (021) 5422 0808 | Fax. (021) 5422 0800